Journal of Materials Chemistry A

TanLee2013

RSC Publishing

FEATURE ARTICLE

View Article Online
View Journal | View Issue

Graphene for supercapacitor applications

Yu Bin Tan and Jong-Min Lee*

Cite this: *J. Mater. Chem. A*, 2013, **1**, 14814

Received 6th June 2013
Accepted 27th August 2013

DOI: 10.1039/c3ta12193c

www.rsc.org/MaterialsA

Graphene has attracted extensive interest in the field of supercapacitor research due to its 2D structure which grants it exceptional properties such as superior electrical conductivity and mechanical properties as well as an extensive surface area better than that of carbon nanotubes (CNTs). Furthermore, unlike other carbon materials, graphene is particularly optimal for supercapacitor applications as its surface area does not vary with pore size distribution and grants electrolyte access to both its surfaces. This article aims to review the advances in recent research and development of the use of graphene for supercapacitor use. The focus would mainly be on the areas of graphene synthesis, graphene modification, graphene–nanoporous carbon composites, graphene–polymer composites and graphene–metal oxides and their potential use in both asymmetric and symmetric supercapacitors. Lastly, the article aims to identify optimal testing methods for electrode performance and choice of electrolytes. It will then stress the increasing need to standardise electrode testing to ensure that test results are as relevant to real life applications as possible.

1 Introduction

1.1 Historical overview and properties of graphene

Graphene is a planar sheet of sp^2 bonded carbon atoms densely packed in a honey comb crystal lattice. It is one atom thick and can be easily obtained from graphite. It also displays favourable electrical, mechanical and morphological properties such as excellent carrier mobility, large spring constant and good Young's modulus value. In addition, its extensive surface area properties that do not vary with pore size distribution make it an attractive choice of material for use in many electronic devices.[1]

The term 'graphene' was introduced in 1986 by Boehm and co-workers and was derived from graphite and the –ene suffix which denotes polycyclic aromatic hydrocarbons.[2] Graphite, in turn, was derived from the Greek word 'graphein' which means 'to write'.[3] Not only did the name of graphene originate from graphite, graphene could also be physically obtained from graphite as graphene is simply the single layer version of graphite.[2] Therefore, as graphene and graphite are closely related, it makes sense that any discussion on the historical elements of graphene should also include graphite and its related compounds (graphite oxide and graphite intercalated compounds). Graphite's first appearance in the literature took place in the early 19th century when Schefhaeutl, a German researcher, recorded the intercalation and exfoliation of graphite using acids.[4,5] This was followed by studies conducted in 1859 by Brodie, a British scientist, who introduced graphite

School of Chemical and Biomedical Engineering, Nanyang Technological University, Singapore 637459, Singapore. E-mail: jmlee@ntu.edu.sg; Fax: +65 6513 8129; Tel: +65 6513 8129

Yu Bin Tan is currently a NTU President Research Scholar in the School of Chemical & Biomedical Engineering at Nanyang Technological University. His research interest lies in the area of using carbon novel materials for electrochemical energy storage and conversion.

Jong-Min Lee received his Ph.D degree at Department of Chemical Engineering at Columbia University in 2003. Since 2008, he has been appointed as an Assistant Professor in School of Chemical and Biomedical Engineering at Nanyang Technological University. His research interests are in development of mesoporous materials for electrochemical energy systems.

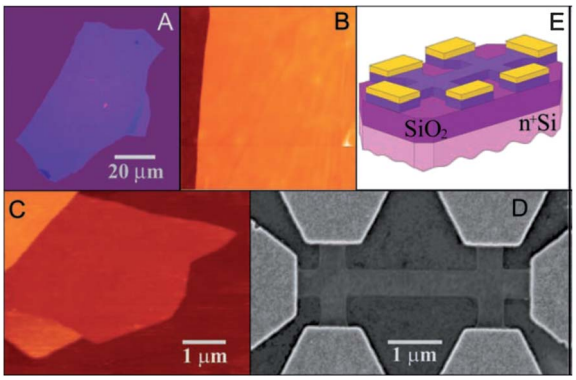

Fig. 1 Graphene films. (A) Photograph (under normal white light) of a relatively large multilayer graphene flake with thickness 3 nm on top of an oxidized Si wafer. (B) Atomic force microscope (AFM) image of 2 μm by 2 μm area of this flake near its edge. (C) AFM image of single-layer graphene. Colors: dark brown, SiO_2 surface; brown-red (central area), 0.8 nm height; yellow-brown (bottom left), 1.2 nm; orange (top left), 2.5 nm. Notice the folded part of the film near the bottom, which exhibits a differential height of ~0.4 nm. (D) Scanning electron microscope image of one of our experimental devices prepared from FLG. (E) Schematic view of the device in (D). Reprinted (adapted) with permission from "Electric field effect in atomically thin carbon films, *Science*, 2004, **306** 666".[16]

to strong acids thus producing graphene oxide with the basal plane filled with both hydroxyl and epoxide functional groups.[6,7]

In the 20th century, a significant number of graphene and graphite related studies were conducted. Of note, in a study conducted by G. Ruess and F. Vogt in 1948 it was observed that graphite oxide suspension was made up of suspended atomic planes and in subsequent investigations in 1962 by U. Hofmann and co-workers monolayers in reduced graphite oxide were identified.[8,9] This preceded a series of papers, in the 1970s, on the growth of thin graphite films on metal substrates, insulating carbides and graphite.[10–14] In 1986, Boehm and co-workers introduced the term 'graphene' and this was later adopted by IUPAC in 1997 in their Compendium of Chemical Technology.[1]

Later in 1990, a study conducted by Kurz and co-workers made use of the familiar technique of mechanical exfoliation of graphite layers with tape for carrier dynamic studies of graphite.[15] This technique was similar to that used in the Nobel-Prize winning study on graphene in 2004.[16] Subsequent research from 1990 to 2004 consisted of SEM photographs of graphite platelets, electrical studies of graphene films and studies of graphene monolayers.[17–19]

However, despite many previous graphite/graphene research studies over the years, it was not until 2004 when the article "Electric Field Effect in Atomically Thin Carbon Films" was published in the Science journal that graphene finally gained worldwide attention.[16] The authors attributed this phenomenon to the fact that unlike previous studies which were highly observational, the research papers in 2004 reported studies on the electrical properties of graphene and showed the world the potential of graphene and its future use in electronics (Fig. 1).[20]

Since the publication of that defining article in 2004, much research has been conducted on graphene to identify its promising electrical, mechanical and morphological properties and its potential use in the areas of fuel cells, lithium batteries and supercapacitors.[2,11] Notably, much emphasis has been placed on research into the large-scale and low cost synthesis of graphene as well as the correlation between the graphene structure and the electrochemical performances needed (Fig. 2 and 3).

1.2 Supercapacitors and their applications

With the ever increasing demand for energy coupled with power shortages and high prices in today's globalised world, there has been a reinvigorated drive to research advanced energy storage and management devices. Supercapacitors have attracted particular attention in light of their excellent power density, fast charging rate and extended cycle life.[22,23] With the current advances in supercapacitors, they could be used for a multitude of purposes such as hybrid electric vehicles, personal electronics and more. At the current rate of research in this field,

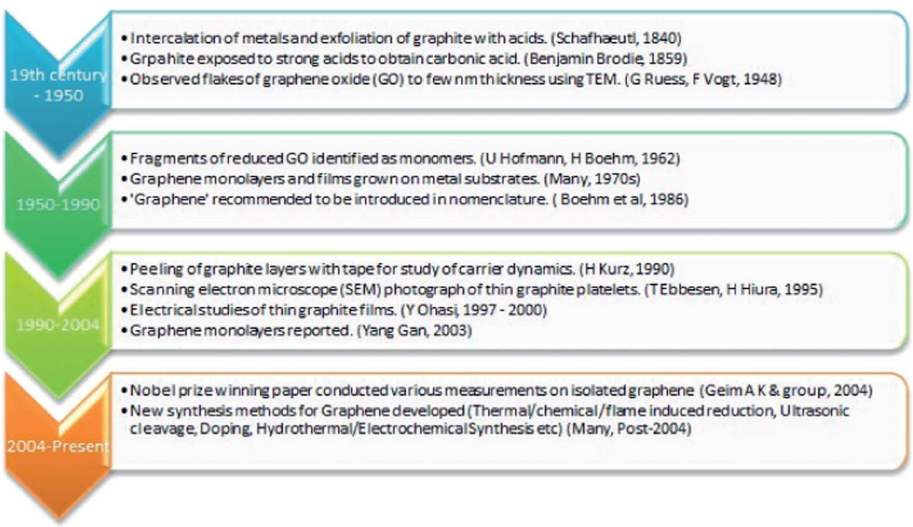

Fig. 2 Flowchart showing the history of graphite/graphene research.

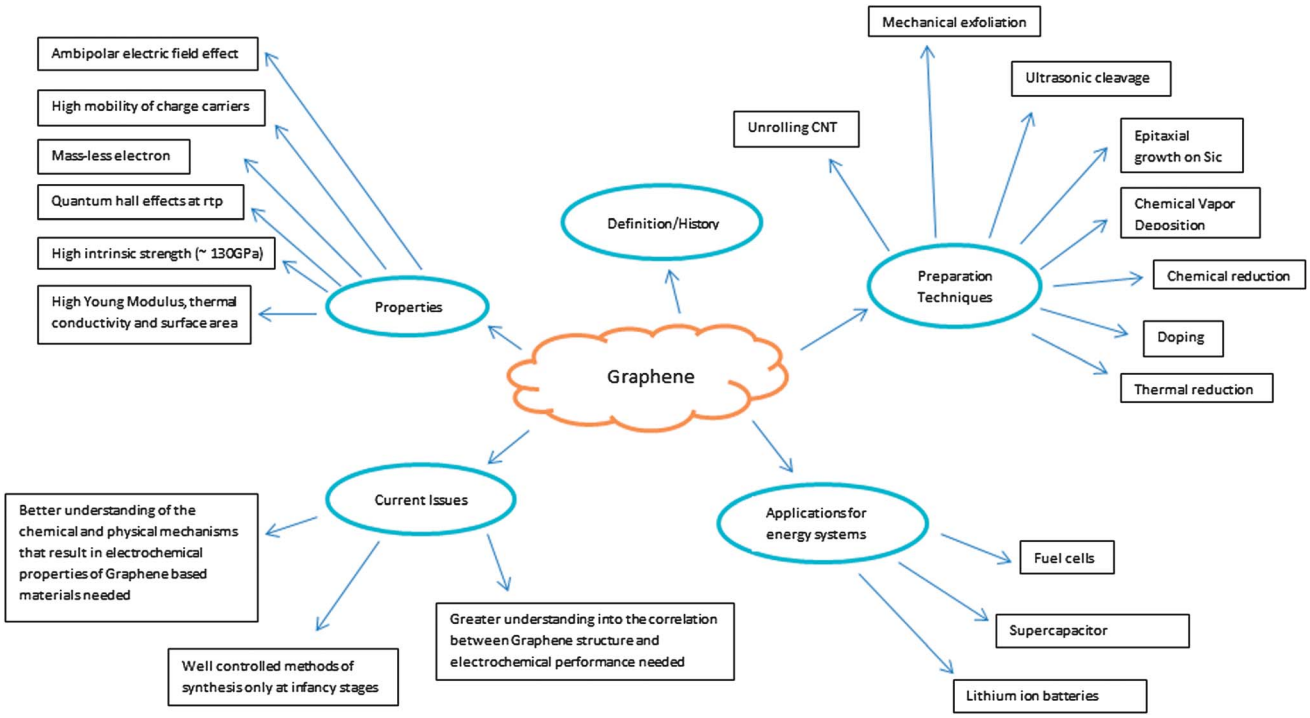

Fig. 3 Graphene research advances mindmap.

supercapacitors currently have higher power densities compared to batteries while their energy densities still lag behind. However, there is optimism that the energy densities of supercapacitors could be eventually improved such that they would be comparable to batteries.

A typical supercapacitor comprises dual electrodes separated *via* a porous separator in an electrolyte medium. When the voltage is supplied, accumulation of opposite charges at the two electrodes would result and these charges would generate an electric field that would allow the supercapacitor to store energy. The main parameters that researchers are interested in are the energy and power densities. Energy density is the ability to store energy and it determines how long the supercapacitor can act as a power source. The energy storage capability of a supercapacitor is represented by the equation below.

$$E = \frac{1}{2}CV^2 \quad (1)$$

where C represents the capacitance. Since the energy density is just simply the energy stored per unit volume or per unit mass and shows a positive linear dependence on the capacitance, therefore much research has been conducted in order to achieve the highest possible capacitance in supercapacitors. Capacitance is the ratio of charge stored to voltage applied and can be represented by the equation below.

$$C = \varepsilon_0\varepsilon_r\frac{A}{D} \quad (2)$$

where ε_0 and ε_r represent the dielectric constants of free space and for the insulating material flanked by the electrodes respectively, A is the electrode surface area and D is the distance between the electrodes. From the equation, it can therefore be observed that one of the main ways to improve the capacitance would be to increase the surface area of the electrodes. As graphene has an extensive surface area, it makes a good candidate as an electrode material.

Lastly, power density is another important parameter of supercapacitors as it determines how fast the energy could be discharged or charged. A high power density for a car that is powered by a supercapacitor would mean that the charging time for the car would be much shorter than that for a conventional battery and the car would also be able to accelerate at faster speeds compared to the power supplied by the battery. The maximum power achievable by the supercapacitor is given in the equation below.

$$P = \frac{V^2}{4\ \mathrm{ESR}} \quad (3)$$

where V^2 represents the voltage and ESR is the equivalent series resistance. As such, another incentive to improving the power density would be to reduce the resistance of the electrode.

Supercapacitors can be categorized into two forms based on their capacitance generating mechanism. The electric double layer capacitance (EDLC) type generates capacitance from the separation of charges at the interface between the electrode and the electrolyte and this attribute can be improved by optimizing the pore volume and size distribution, hierarchical structure and interconnectedness between macropores and mesopores as well as by expanding the specific surface area of the material. Due to the nature of EDLC, charges are not transferred between the electrode and the electrolyte thus making charge storage highly reversible and this increases the cycling stability of the supercapacitor.[24] The pseudocapacitance, on the other hand,

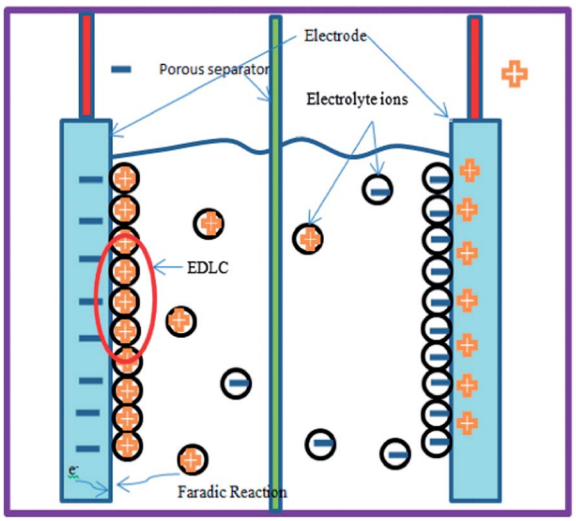

Fig. 4 Schematic showing 2 cell electrode configurations with both EDLC and pseudocapacitance.

generates capacitance from rapid Faradaic reactions within the electrode material.[25,26] These fast faradaic reactions may include redox reactions, intercalation and electrosorption processes.[24] EDL capacitors have good electrochemical cyclic stability, but their capacitance value is often low. Pseudo-capacitors exhibit high capacitance but relatively poor cyclic stability. Comprehensive utilization of EDL and pseudo-capacitor electrode materials has been confirmed to be an effective method by which high performance may be achieved (Fig. 4).

Graphene, known for its constant surface area and pore size distribution as well as good surface exposure to electrolytes, has been recognised as an excellent component for supercapacitors.[27] Other incredible properties of graphene include high thermal conductivity of up to 5000 W m^{-1} k^{-1}, great strength with a Young's modulus of around 1 TPa and extensive surface area with a theoretical value of 2630 m^2 g^{-1}.[28] As this literature review aims to study the recent advances in graphene science towards supercapacitor use, it is imperative that the main parameters that describe a good supercapacitor be discussed.

The first and arguably most important factor that determines the capacitance and, by extension, the supercapacitor performance is the effective surface area. The effective surface area determines how large the electrode/electrolyte interface is and thus how extensive EDLC will be. Although graphene has an extensive theoretical surface area, this area will not result in high EDLC if it is not ion-accessible. Therefore it should be noted that the capacitance is largely dependent on the layering and stacking configuration of graphene and much research has been conducted to create graphene composite structures that display large ion accessible surface areas.

Porosity, along with pore volume and pore size distribution, also plays an important role in the capacitance of an electrode. The pore size typically determines the type of ions that are accessible to the surface of the electrode. It is essential to optimize this variable such that most of the electrolyte ions can reach the surface for optimal performance. The optimal pore size and volume are also largely dependent on the type of

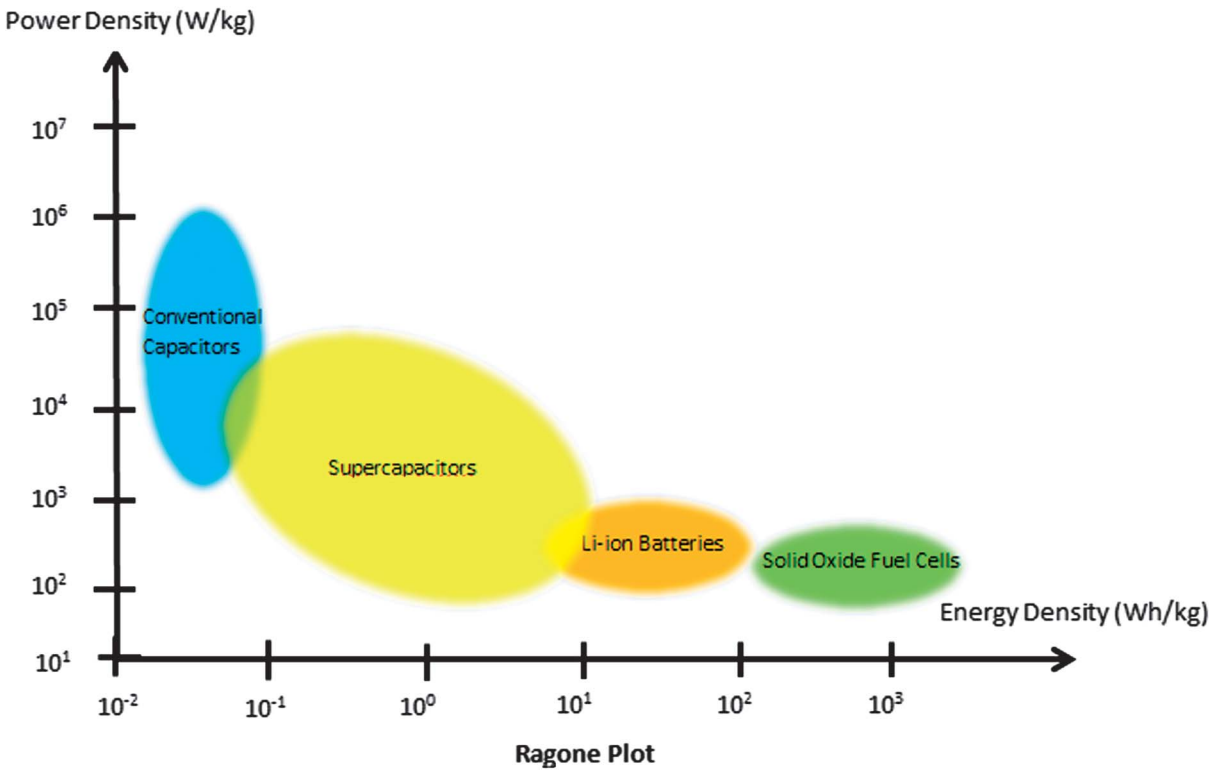

Fig. 5 Ragone plot.

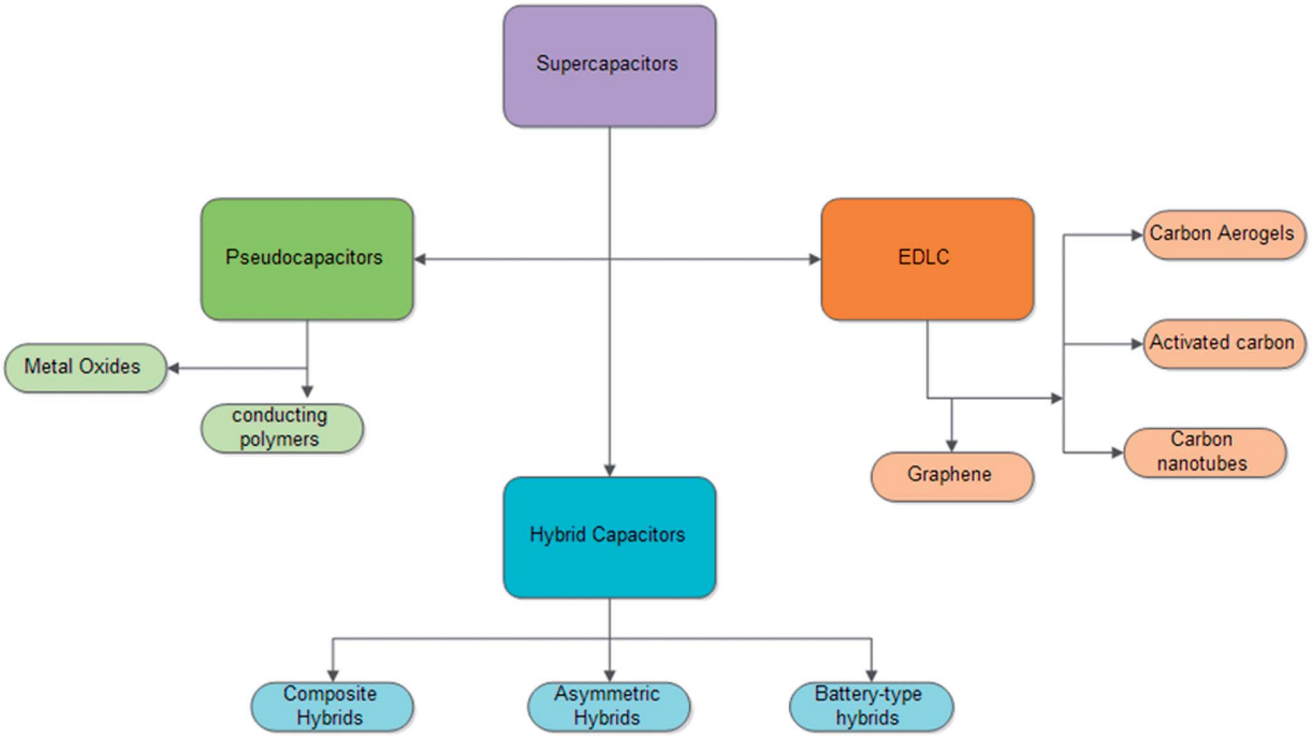

Fig. 6 Chart showing types of supercapacitors.

electrolyte used. For example, it has been shown that for a pore size of <1.5 nm the surface is inaccessible to most ionic liquids. The total pore volume, on the other hand, has to be small to allow for the electrode to be densely packed so that it can be as light as possible.

Other factors such as the internal resistance between graphene sheets (measured by a Nyquist plot), functional groups on the graphene surface, surface wettability, edge effects and cycling ability also help determine the supercapacitor performance.

1.3 Objectives

The objective of this article is to review recent advances in graphene synthesis and its possible limitations. In addition, it will aim to illustrate as many novel methods of graphene synthesis for supercapacitor applications as possible. As previously mentioned, supercapacitors have lower energy densities than batteries. This could be resolved by either using novel electrode materials to increase the capacitance or by using electrolytes with larger electrochemical potential windows. Therefore, this review article would also focus on the five main research areas for improving graphene use as electrodes in supercapacitors for superior capacitance. They include (1) graphene–nanoporous carbon composites; (2) graphene modifications; (3) graphene–polymer hybridization; (4) graphene–metal oxide composites and (5) graphene in asymmetrical supercapacitors. Lastly, the article aims to identify optimal testing methods for electrode performance and choice of electrolytes. It will then stress the increasing need to standardise electrode testing to ensure that test results are as relevant to real life applications as possible.

Unlike other review articles such as "graphene-based electrodes for electrochemical energy storage" written by Xu *et al.*[29] and "graphene-based electrochemical energy conversion and storage: fuel cells, supercapacitors and lithium ion batteries" written by Hou *et al.*,[21] this review article gives an in-depth review on the graphene utility for supercapacitors. In addition, whereas these review articles cover the typical areas of graphene synthesis, graphene modifications, graphene polymer hybrids and graphene metal oxide composites, this article goes further in covering graphene–nanoporous carbon composites in detail as well as reviewing the optimal testing methods for electrode performance and the important choice of electrolytes which are vital components that should also be discussed in a comprehensive review of the utility of graphene for supercapacitor applications (Fig. 5 and 6).

2 Review of graphene synthesis methods

There are many methods to prepare graphene and the method used will depend on the final function that graphene needs to achieve. In addition, multiple methods of graphene synthesis might be needed to unleash the full potential of graphene. There are two general ways in which graphene can be synthesized. The first involves synthesis of graphene sheets by dismantling from graphite. The second involves synthesis of graphene from other carbon sources such as carbon nanotubes.[28] Among the many methods for synthesizing graphene, mechanical exfoliation and chemical vapor deposition (CVD) have the ability to produce good quality single layer graphene films but are often low yielding. By comparison, liquid-phase exfoliation holds great promise as the graphene obtained from

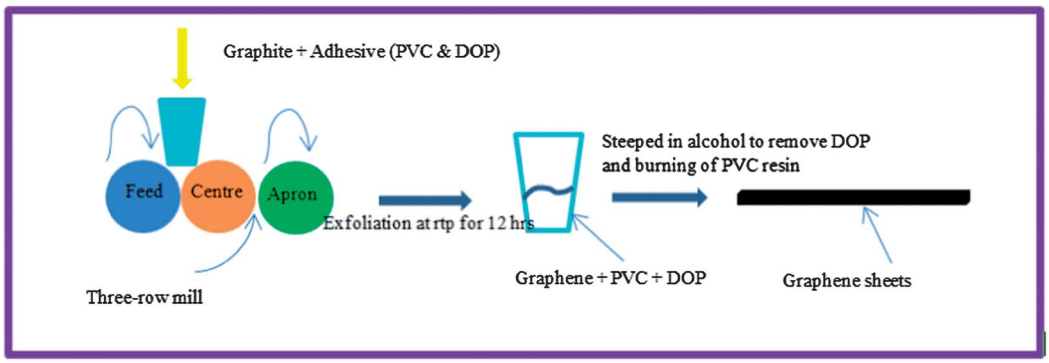

Fig. 7 Schematic of continuous mechanical exfoliation of graphene as invented by J. Chen and co-workers.

graphene oxide (GO) displays excellent connectivity among the electrolyte and electrode materials due to the hydrophilic reduced GO. In addition, this method also provides much potential for mass production.[30] There are also many other methods for synthesizing graphene and the more significant methods for graphene synthesis will be discussed below.

2.1 Mechanical exfoliation

As discussed in the 'historical overview of graphene' section, the earliest method for producing graphene was through mechanical exfoliation using tape. This was conducted by Kurz and co-workers in 1990 and was subsequently repeated by Geim and co-workers in their defining study in 2004.[15,16] Geim and co-workers' approach on pyrolytic graphene was found to be efficient and easily repeatable in generating few-layer graphene (FLG) of 10 μm thickness. In addition, common materials such as scotch tape could be used for the peeling process and Gein himself described the process as "so straightforward and accessible that even school children could probably do it".[20] Advantages of this method include the ability to produce high quality graphene typically used for laboratory research due to little graphene processing steps required. However, limitations for this method include its unsuitability for large scale production as it is slow and labour intensive. J. Chen and co-workers attempt to resolve this limitation by investigating a novel continuous mechanical exfoliation process (Fig. 7). This process uses a three-roll mill machine, common in the rubber industry, to produce single/few-layer graphene from natural graphite. This approach could also be used to prepare graphene–polymer composites and could be further enhanced by using the right types of polymer adhesives as well as rolling time, temperature and speed of rolling.[31]

2.2 Liquid phase exfoliation

Similar to mechanical exfoliation, graphite can be exfoliated in water or organic solvents and with the use of proper surfactants. Ultrasonic agitation would then be used to supply the energy needed to cleave the graphene from its precursors.[21] One of the reasons for research into such solvent-based exfoliation is the increasing demand for a process that would produce graphene using a large-scale and efficient process. The initial search for such a process involved the use of water which was used as a solvent to exfoliate graphite oxide to form aqueous layers of graphene oxide (GO). This idea was thought to be good as the morphological and chemical properties of the GO made it extremely stable in water. However, disadvantages of this method include the poor electrical conductivity of GO as a result of the disruption in the π orbital structure during oxidation. Simply reducing GO would not resolve any of the morphological defects that made GO a poor electric conductor.[32–35]

In view of the limitations of exfoliation of graphite oxide, studies have been conducted to exfoliate graphite instead. As discussed by Coleman, the similarities in surface energy between nanotubes and graphene suggest that *N*-methyl-2-pyrrolidone (NMP) could be used to exfoliate graphite to graphene.[36] This solvent-assisted method allowed the synthesis of non-defective graphene. Another possible approach was to use water as a solvent. However, this approach requires the use of surfactants as water does not meet the requirements of a solvent for graphene due to its surface energy properties. Surfactants such as sodium dodecylbenzene sulphonate (SDBS) could be used and this relieves us of the need to use high boiling points or toxic solvents such as NMP.[36,37]

2.3 Chemical vapour deposition

Chemical Vapour Deposition (CVD) is a chemical process that allows gaseous reactants to be deposited on a substrate to produce materials that are superior in purity and performance. In this case, graphene can be prepared on metallic surfaces through CVD. In a recent study, gaseous ethylene was deposited on a hot Ir surface through CVD to produce graphene sheets with superior morphological properties.[38] Another study used the metal Ruthenium as a substrate for the epitaxial growth of crystalline monolayer graphene using CVD.[39] 3D graphene networks could also be synthesized *via* the CVD process. An investigation into this novel process made use of Ni foam as a template and ethanol as the carbon source. The prepared graphene has a unique 3D configuration that allows rapid access to electrolytes due to its large surface area. In addition, by directly synthesising graphene onto the Ni current collector, this would allow rapid transfer of charges from the active materials to the current collectors through the graphene 3D configuration.[40] Notably, CVD synthesis of graphene should not be conducted on flat metal surfaces or thin films to avoid problems of low

yield. Furthermore, depending on the metal on which graphene is grown, optimal conditions for CVD varies. Other metals on which graphene can be grown *via* CVD include Co, Rh, Pd, Pt, Cu, Au and a number of other alloys such as Co–Ni, Au–Ni, Ni–Mo and stainless steel.[28]

2.4 Epitaxial growth on metal surfaces

Epitaxial growth of graphene on metallic surfaces has been explored as a synthesis method that may overcome the limitations of other synthesis methodologies such as mechanical exfoliation where the size, structure and film thickness cannot be uniformly controlled.[41] This technique of synthesizing graphene often go hand-in-hand with CVD as CVD is needed to deposit the C molecules on the metal surfaces. The initial research on epitaxial growth of graphene focused on silicon carbide (SIC). Graphene growth on SIC allows development of graphene devices that can function at room temperature and film transfer is unnecessary.[28] However, SIC surfaces are expensive and can lead to difficulties in transferring graphene to other substrates thus resulting in further research into other metallic surfaces such as Ru, Ir, Cu, Pt and Ni thin films.[41,42] One of the main variables that can impact the quality of graphene grown is the growth temperature. For example, graphene has been epitaxially grown on Pt(111) and it was discovered that the graphene quality is highly correlated with the growth temperature and ethylene exposure.[42] Similarly, the temperature for CVD is significant to the quality of graphene grown on a Cu(111) film.[41] For example, at a CVD temperature of 1000 °C, high quality graphene was grown while at 900 °C, lower quality graphene was produced.[41] Other efforts are also ongoing to use a cheaper and easily available free-standing polycrystalline 3C–SiC for graphene growth *via* solid state graphitization.[43]

2.5 Chemical reduction

Similar to thermal reduction, chemical reduction involves the use of both oxidation and reduction to produce graphene sheets from graphite. The process is rather simple. Firstly, graphite is oxidised into graphite oxide and then exfoliated into graphene oxide sheets. Next, reduction of these graphene oxide sheets to graphene occurs.[21] However, in order to ensure that the reduction is a success, the appropriate reducing agent, solvent and surfactant must be used. This would help produce a stable suspension. Based on research, it has been discovered that hydrazine hydrate is one of the most effective reducing agents.[44] Despite this, hydrazine hydrate and most other reducing agents are toxic or generate hazardous byproducts. As such, studies have been conducted to discover non-hazardous ways to reduce graphene oxide to graphene. One such research used an alkaline hydrothermal process to reduce graphene oxide.[45] It was reported that this method was successful in producing graphene that had similar morphological properties to those produced *via* the hydrazine reduction method. Another

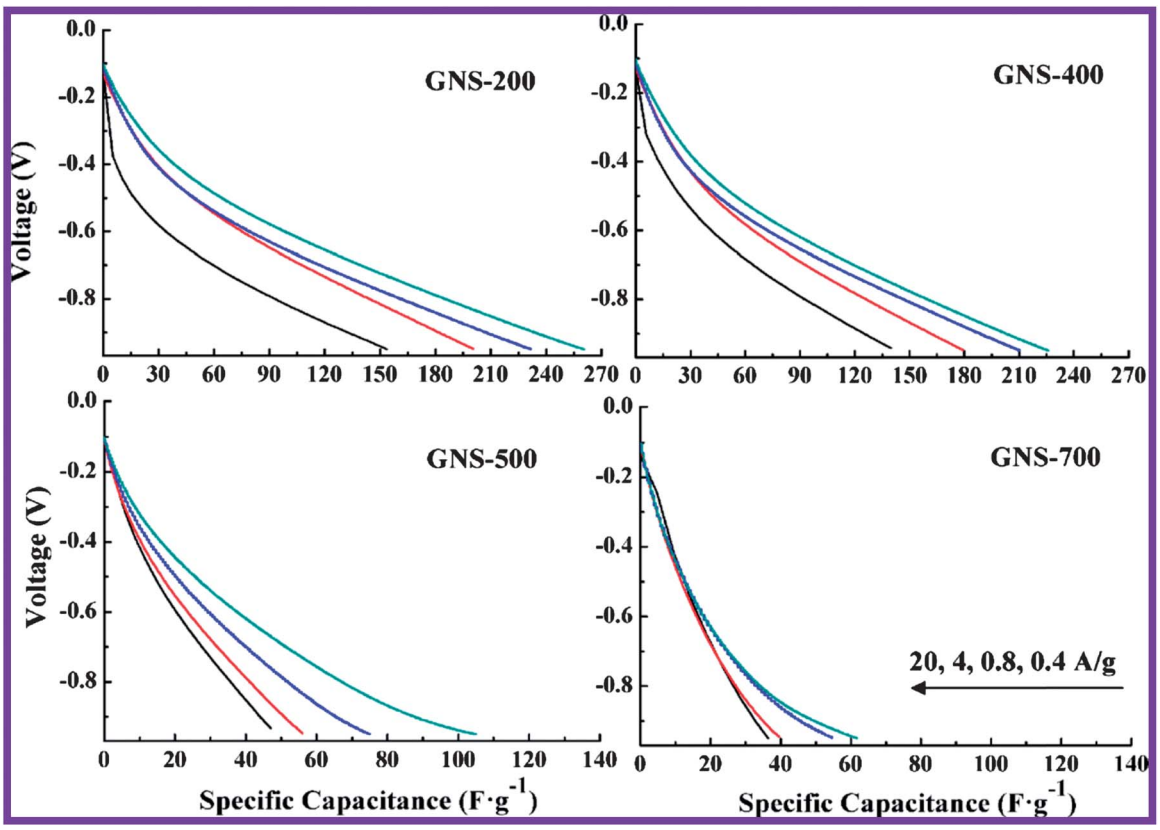

Fig. 8 Discharge curves obtained in 6 M KOH for GNS-200, GNS-400, GNS-500 and GNS-700 at different current densities. (Reprinted from *J. Power Sources*, 2012, **198**, 423–427, with permission from Elsevier).[47]

problem in such hydrazine-based reduction methods is the tendency of separated graphene sheets to re-amalgamate together. Methods to prevent this has been studied and it was discovered that when high ionic KCl solution is introduced into the reduction process, the buoyancy and repulsive force from the ions prevent the graphene sheets from re-stacking to each other after it was reduced thus producing highly flaky graphene sheets with higher specific capacitance.[46]

2.6 Thermal reduction

Thermal reduction of graphene involves the 2 stages of acid and heat treatment. For thermal expansion to happen, sufficient oxidation is needed during the acid treatment stage while an appropriate amount of pressure is needed for the thermal heat treatment stage. Graphite is eventually separated into graphene sheets when the pressure builds up between the graphite layers due to a high decomposition of the epoxide and hydroxyl functional groups that have been introduced onto the graphite surface as a result of oxidation. This pressure must be able to overcome the inherent van der Waals forces that exist between the layers before separation can occur.[21] Interestingly, a recent study highlighted that the optimal temperature for thermal reduction is 200 °C as shown in Fig. 8. The study tested thermal reduction of graphene oxide to produce graphene sheets (GNS) from 200–900 °C and it was discovered that graphene produced at 200 °C showed the highest capacitance of 260.5 F g^{-1} at a current density of 0.4 A g^{-1} as shown in Fig. 9. In addition, it was discovered that the amount of oxygen containing groups was the main factor in influencing the capacitance performance of these graphene sheets.[46]

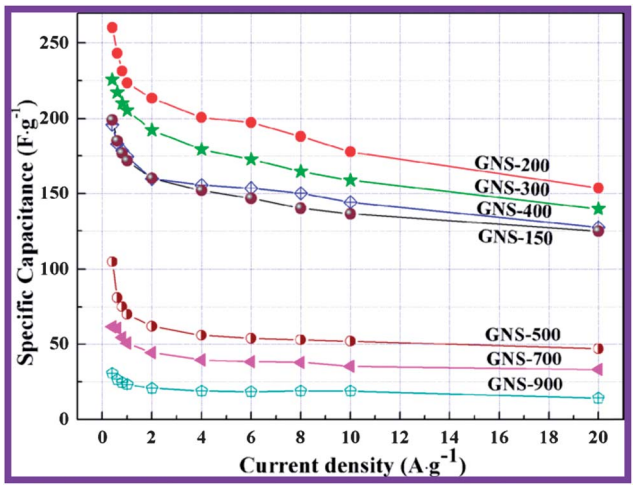

Fig. 9 Rate capacitances of the samples in 6 M KOH with different current densities. (Reprinted from *J. Power Sources*, 2012, **198**, 423–427, with permission from Elsevier).[47]

2.7 Flame-induced reduction

Reduced graphene oxide can be easily produced *via* the use of a simple flame from a common lighter to reduce graphene oxide. This process is quick, clean, cheap and easy to complete without the need for any reducing agent. In addition, such a process retains the oxygen containing functional groups on its surface as well as increases the functional surface area of the graphene oxide paper. These traits are beneficial for increasing the conductance of the material (Fig. 10).[48]

2.8 Electrochemical synthesis

The synthesis of reduced graphene oxide *via* electrochemical methods has been studied and shown to produce superior supercapacitor materials with a specific capacitance of 128 F g^{-1} and a cycling retention of 86% after 3500 cycles. This method involved the use of constant potential and also allows the control of experimental variables such as the applied voltage and current as well as the reduction time. In addition, the width and thickness of the graphene oxide film can also be controlled *via* the degree of deposition of the graphene oxide on the electrode.[49]

2.9 Unrolling of carbon nanotubes

Carbon nanotubes can be unrolled and exfoliated to produce graphene. Several studies have been conducted to this end and involve electrostatic attraction between opposing ion charges, strong oxidising agents or even an Ar plasma etching method. For the electrostatic approach, Li ions in an NH_3 solvent were intercalated between the layers of multiwall carbon nanotubes (MWCNTs) through electrostatic attraction between the positive Li ions and the negative MWCNTs. This causes the MWCNT

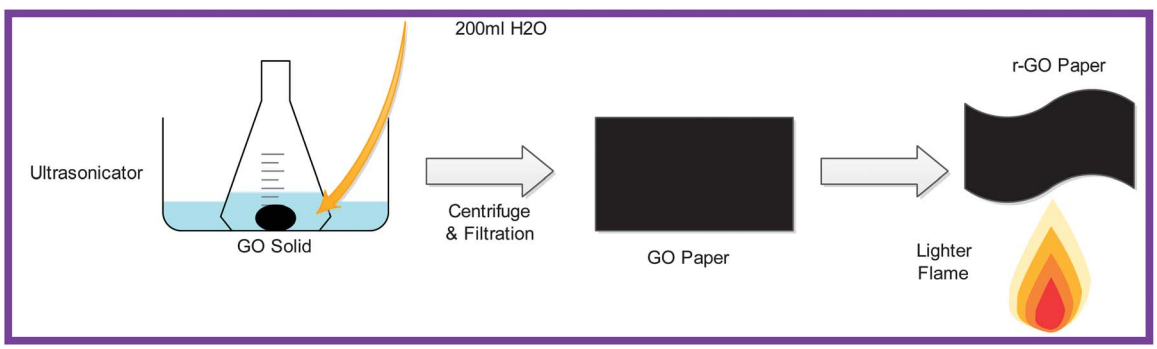

Fig. 10 Using a lighter flame to prepare r-GO paper.

layers to disperse and the walls to eventually rupture. The ruptured MWCNT is then further treated with HCl and heat to increase the degree of exfoliation.[50] Separately, strong oxidising agents such as $KMnO_4$ in a solution-based oxidising approach could be used to 'unzip' MWCNTs to form nanoribbons. This approach is based on alkene oxidation by the oxidising agent (in this case $KMnO_4$) and results in the formation of esters and diones. The positioning of these ketones further weakens the alkene structure thus resulting in an increased susceptibility to further oxidative attacks and eventually leads to a 'tear' in the MWCNTs.[51]

2.10 ARC discharge

Traditionally, this method has been used to synthesize other carbon-based nanomaterials such as CNTs by passing a current through high purity graphite electrodes. However, more recently, this method has been utilized to produce few-layer graphene in the presence of a number of buffer gases. Hydrogen and helium gases are examples of the types of buffer gases needed and a mixture of these gases was found to produce the highest crystallinity material.[28]

3 Graphene-based electrodes for supercapacitors

3.1 Graphene–nanoporous carbon supercapacitors

In recent studies, nanoporous carbon materials have been combined with graphene to investigate the effects of porosity on the supercapacitor performance. Nanoporous carbon materials are typically derived from carbide and can take the form of structures that differ in their degree of porosity. Depending on the method of formulation, a degree of microporous and mesoporous structures can be formed and the pore volume, size and size distribution can be carefully controlled.

One such study where graphene–nanoporous carbon composites were used to study the impact of porosity on the supercapacitor performance was conducted by Bandosz *et al.*[52] In this study, nanoporous carbon derived from poly(4-styrenesulfonic acid-*co*-maleic acid) sodium salt (PS) was prepared with 5% and 20% graphene separately. The experiments were carried out with 1 M H_2SO_4 and 0.5 M Na_2SO_4 in both 2 and 3 cell electrode configurations. It was discovered that a pore volume of less than 0.7 nm was highly effective for EDLC and produces the highest gravimetric capacitance when tested against other pore volumes of 1 nm and 2 nm. In addition, it was discovered that Na_2SO_4 exhibited a higher performance in capacitance at the corresponding pore volumes and this can be attributed to the greater pseudocapacitance effects in Na_2SO_4. It is known that the pseudocapacitance can have a greater significant effect on the capacitance at larger pore volumes due to the increased probability of functional groups existing. The author also defined the term "active pore space utilization" which is used to signify the ratio of capacitance to pore volumes less than 0.7 nm. It was discovered that the active pore space utilization increased with increasing graphene content within the composite and it is also directly dependent on the conductivity of the composites.[52] This study suggests the importance of pore volumes and graphene content in the design of supercapacitor electrodes. Pore volumes must be optimized to less than 0.7 nm and graphene should be introduced for improved conductivity to achieve the best possible capacitance performance (Fig. 11).

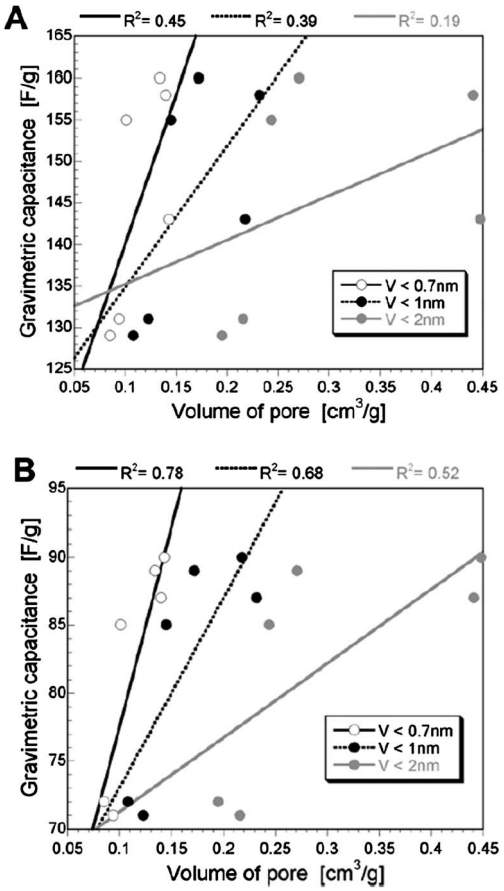

Fig. 11 Dependence of the capacitance in H_2SO_4 (A) and Na_2SO_4 (B) on the volume of the pores of different sizes. Reprinted (adapted) with permission from "active pore space utilization in nanoporous carbon-based supercapacitors: effects of conductivity and pore accessibility" Elsevier.[52]

However, it must be noted that although both these factors are important and necessary for improving the capacitance performance, the pore volume seems to be the main factor in influencing the capacitance. This has been proven in an earlier study also conducted by Bandosz *et al.*[53]

Much research has also been conducted into other graphene–nanoporous carbon materials such as carbon nanotubes (CNTs) and carbon fibres (CFs).[54] The purpose of developing these novel composites was often to increase the effective surface area or functional groups with oxygen on the surface of graphene as these are important factors that increase the capacitance of supercapacitors. One way to increase the effective surface area is to prevent the aggregation of graphene sheets. The aggregation would prevent ions from reaching the inner layers of graphene thus preventing electrochemical double layers from forming and reducing the specific capacitance in the process.

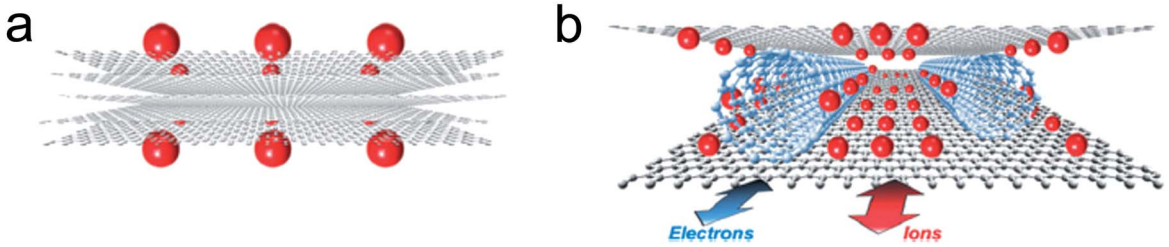

Fig. 12 (a) Pristine graphene that is susceptible to aggregation (b) graphene–CNT composite that acts as spacers and binders. Reprinted (adapted) with permission from "graphene and carbon nanotube composite electrodes for supercapacitors with ultra-high energy density, *Phys. Chem. Chem. Phys.*, **2011**, 13, 17615–17624" PCCP.[55]

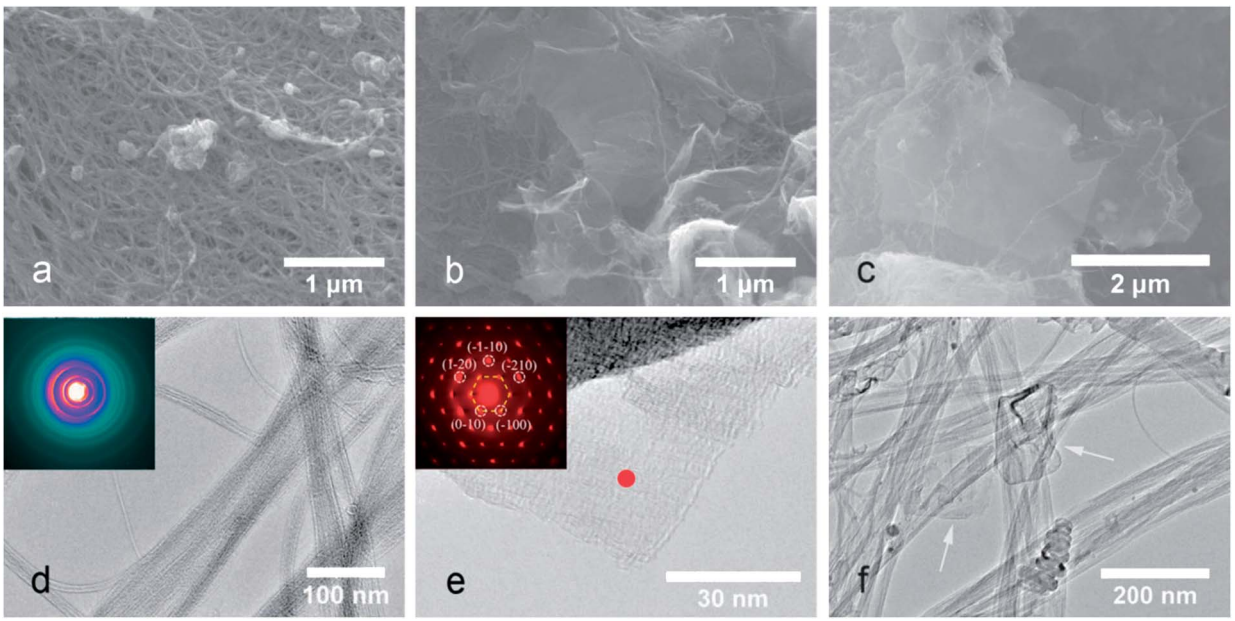

Fig. 13 Morphological and structural characterization of various carbon electrodes. (a) SEM image of the CNT film. (b) SEM image of the graphene–CNT composite at low magnification. (c) SEM image of the graphene–CNT composite at high magnification. (d) TEM image of CNTs. Inset is an electron diffraction pattern. (e) TEM image of the prepared graphene. Inset is an electron diffraction pattern acquired at the location indicated in the image. (f) TEM image of the graphene–CNT composite. Reprinted (adapted) with permission from "graphene and carbon nanotube composite electrodes for supercapacitors with ultra-high energy density, *Phys. Chem. Chem. Phys.*, 2011, **13**, 17615–17624" PCCP.[55]

Recent research shows how aggregation of graphene sheets can be prevented through the use of carbon nanotubes as spacers.[55] Graphene sheets tend to aggregate during the drying process as a result of van der Waals interactions. Thus ions would have difficulty accessing the pores of the graphene especially at high charging rates. As CNTs have excellent conductivities, surface area and mechanical properties, they make ideal spacers as shown in Fig. 12. This also leads to the reduction of resistance within the electrode. Furthermore, CNTs can also act as binders to hold the graphene sheets together. Results showed that the graphene–CNT electrodes outperform pure CNTs or graphene electrodes with calculated specific capacitances of 290.4 F g^{-1} and 201.0 F g^{-1} in KCl and $TEABF_4$ electrolytes respectively. This could be attributed to the increase in surface area to 421.3 m^2 g^{-1} as measured by the Brunauer–Emmett–Teller (BET) method. In addition, when the cycling ability of CNT–graphene was tested to determine the durable properties of the electrode, it was found that 'electro-activation' occurred (Fig. 13).[56]

Electroactivation is a phenomenon where graphene sheets would allow better access to different ions through positional adjustments. In addition, long cycling time typically allows ions to intercalate between graphene sheets thus preventing aggregation and increasing the surface area for other ions to access. This meant that despite the 1300 complete charging–discharge cycles, the specific capacitance of the graphene–CNT electrodes actually improved. The advantages of such modifications to graphene are manifold. As compared to activated carbon which is currently the most popular material for supercapacitors, graphene–CNT electrodes of this structure would significantly allow electrolytes to access more carbon atoms thus improving the performance of the supercapacitors. Potential future applications that could benefit from the improvements in capacitance as well as electrical conductivity when graphene–CNT is

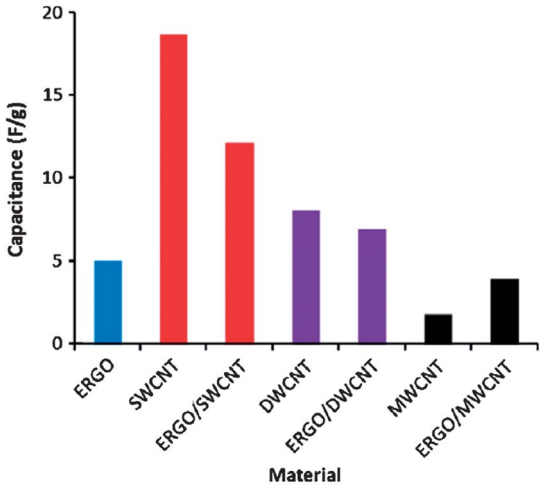

Fig. 14 Weight specific capacitances of pure reduced graphene (ERGO), pure carbon nanotubes (SWCNT, DWCNT and MWCNT) and their respective composites. Reprinted (adapted) with permission from "graphene–carbon nanotube composites not exhibiting synergic effect for supercapacitors: the resulting capacitance being average of capacitance of individual components" Elsevier.[57]

used in place of activated carbon include energy storage and saving devices.

Interestingly, a recent study conducted by Pumera *et al.* demonstrated that the use of CNTs as spacers to prevent the aggregation of graphene sheets will not lead to a synergistic effect between the graphene and the CNTs.[57] Instead, the capacitance produced is an approximate average between the two materials. For instance, when exfoliated reduced graphene oxide (ERGO) was mixed with single wall carbon nanotubes (SWCNTs), the achieved weight specific capacitance is 12.1 F g^{-1} which is between the weight specific capacitances of ERGO (4.99 F g^{-1}) and SWCNT (18.6 F g^{-1}). This experiment was carried out with an equal mass ratio of ERGO and SWCNT and similar results were obtained when double wall and multi-wall carbon nanotubes were used. This is in contrast to previous studies conducted which showed that graphene–CNT composites do not necessary lead to increased capacitance. This experiment was conducted by the simple mixing of both ERGO and CNTs. This suggests that more elaborate synthesis methods are required to allow for specific structure configurations of graphene–CNT composites to show superior capacitance performances (Fig. 14).

Another study addresses the multiple issues of interfacial resistance, surface area, pore volume and edge effects through the use of graphene-like carbon fibre paper with surface grown CNTs.[64] The good electrical conductivity and standing structure of the carbon fibres and CNTs would lead to reduced resistance as well as increased surface area and pore volume. These standing structures would also show numerous edge effects thus increasing the specific capacitance.

Similar to the previous experiment, Matsushima *et al.* used a pulsed plasma CVD technique to create nanoporous carbon films containing graphene to use as electrodes for EDLC.[58] For this synthesis process, a metal catalyst, in this case Ni, is required. A carbon precursor and heat energy are other necessary requirements. When the porous graphene films were grown on Ni films that have 50 nm thickness, the capacitance was discovered to be approximately 13 μF cm^{-2}. However, when the thickness of the Ni surface was increased from 50 nm to 100 nm, the capacitance increased to 152 μF cm^{-2}. This significant increase was attributed to the breaking of the Ni surface into larger particles due to the increase in thickness and this facilitated the absorption of carbon atoms resulting in the formation of more desirable graphene structures. The authors concluded that their experiment showed how graphene–nanoporous carbon composites are suitable materials for electrodes in EDLCs but cautioned that the results in this study are not optimised and a more elaborate study could be conducted to better determine the relationship between the thickness of metal catalyst surfaces during the synthesis step and the capacitance performance of the final electrode.[58]

Meanwhile, in a departure from the use of nanoporous carbon materials with graphene, Zhao *et al.* investigated mesoporous carbon spheres (MCS) and found them to exhibit good performance in both aqueous and organic electrolytes.[59] The MCS used in this experiment contains graphene sheets in small domains and has a particle size of 65 nm with a pore diameter of 2.7 nm and a pore volume of 2.9 cm^3 g^{-1}. When the capacitance was measured in the $TEABF_4$ electrolyte, a specific capacitance of 180 F g^{-1} was achieved with an energy density of 62.8 W h kg^{-1} at a power density of 0.16 kW kg^{-1}. The authors attribute this good capacitance performance to the structure of the graphene–MCS composite which exhibited high effective surface area and short diffusion length and this resulted in low diffusion resistance and better capacitive performances (Table 1).[59]

3.2 Modified graphene supercapacitors

In recent research, graphene has often been modified for use in supercapacitors. Such modifications include the idea of using few layer graphene, corrugated graphene sheets, doping of nitrogen onto graphene as well as the preparation of extremely thin graphene sheets. These modifications often serve the aim of improving the capacitance of electrodes through increasing the effective surface area by reducing graphene aggregation (Table 2).[60]

One research study has expanded the idea of single/few layer graphene (FLG).[61] It is believed that with fewer layers, there would be a lower likelihood of aggregation. In this study, FLG was synthesized *via* intercalation of graphite and pre-graphite oxide followed by the reduction of graphite oxide. Such FLG produced a specific capacitance of 180 F g^{-1} in 1 M Na_2SO_4 with a BET measured area of 1400 m^2 g^{-1}. A key limitation in using graphite oxide produced from oxidised graphite includes significant defects which are irreversible and this reduces the electrical conductivity of the electrode produced. Looking ahead, one of the key research areas is the discovery of novel synthesis methods that can produce single/few layer graphene in bulk quantities and without the presence of defects that would reduce its superior electrochemical properties.

Table 1 Summary of research results for graphene–nanoporous carbon supercapacitors[a]

Preparation method	Nature of electrode	Electrode configuration	Mass/SA of electroactive materials	Electrolyte	Measurement protocol	Maximum capacitance (F g^{-1})	Capacitance retention	Ref. (year)
Blending process (sonication)	Graphene and SWCNT	2 Electrode configuration	1 mg (421 m^2 g^{-1})	1 M KCl	CV (ν = 10 mV s^{-1}), (0.5 A g^{-1})	290.6	118% (1300 cycles)	55 (2011)
Blending process (sonication)	Graphene and SWCNT	2 Electrode configuration	1.6 mg (421 m^2 g^{-1})	1 M $TEABF_4$	CV (ν = 10 mV s^{-1}), (0.5 A g^{-1})	201.0	129% (1300 cycles)	55 (2011)
CVD	Graphene–CNT	3 Electrode configuration	Small	—	CV (ν = 10 mV s^{-1})	653.7 μF cm^{-2}	—	56 (2012)
Electrospinning and carbonization	Graphene-like carbon fiber and CNT	3 Electrode configuration	111 m^2 g^{-1}	0.5 M H_2SO_4	CV (0.5 mA cm^{-2})	176	—	64 (2012)
Carbonized and heated	Graphene (20%)–PS	2 Electrode configuration	6–9 mg	0.5 M H_2SO_4	CV (ν = 5 mV s^{-1})	102	65%	52 (2012)
Carbonized and heated	Graphene (20%)–PS	2 Electrode configuration	6–9 mg	0.5 M Na_2SO_4	CV (ν = 5 mV s^{-1})	67	47%	52 (2012)
Simple mixing of graphene and CNT	Graphene–SWCNT, graphene–DWCNT, graphene–MWCNT	3 Electrode configuration	0.5 μg of graphene and 0.5 μg of CNT	0.5 M KCl	CV	SWCNT (12.1 F g^{-1}) DWCNT (6.9 F g^{-1}) MWCNT (1.8 F g^{-1})	—	57 (2012)
Pulsed discharge plasma-CVD	Graphene–carbon nanofibres	2 Electrode configuration	—	2.5 g l^{-1} KOH	CV	152 μF cm^{-2}	—	58 (2012)
CVD	Mesoporous carbon spheres with graphene	2 Electrode configuration	7.0 mg cm^{-2}	1.5 M $TEABF_4$	CC (0.25 A g^{-1})	180 F g^{-1}	78% (700 cycles)	59 (2011)

[a] CV = cyclic voltammetry, CC = galvanostatic charge–discharge.

Table 2 Summary of research results for graphene modified supercapacitors

Preparation method	Nature of electrode	Electrode configuration	Mass/SA of electroactive materials	Electrolyte	Measurement protocol	Maximum capacitance (F g^{-1})	Capacitance retention	Ref. (year)
Intercalation and reduction	Few-layer graphene	3 Electrode configuration	2.5 mg (1400 m^2 g^{-1})	1 M Na_2SO_4	CV (ν = 60 mV s^{-1}), (6 A g^{-1})	180	—	61 (2012)
Thermal reduction	Highly corrugated graphene	3 Electrode configuration	3–4 mg cm^{-2} (518 m^2 g^{-1})	6 M KOH	CV (ν = 2 mV s^{-1})	349	108% (5000 cycles)	62 (2012)
Sonication with KOH	KOH modified graphene	3 Electrode configuration	492 m^2 g^{-1}	1 M Na_2SO_4	CV (ν = 10 mV s^{-1})	136	—	63 (2011)
Intercalation and hydrazine reduction	TBAOH stabilized graphene	3 Electrode configuration	5 mg	2 M H_2SO_4	CV (ν = 100 mV s^{-1}), (1 A g^{-1})	194	90% (1000 cycles)	65 (2011)
Vacuum filtration	Ultrathin graphene	3 Electrode configuration	—	2 M KCl	CC (0.75 A g^{-1})	135	—	67 (2010)
Chemical Vapor Deposition (CVD)	3D pillar graphene nanostructure	2 Electrode configuration	563 m^2 g^{-1}	HNO_3–IPA (67% HNO_3–IPA = 1 : 4)	CV (ν = 100 mV s^{-1})	330	—	68 (2011)
Hydrothermal process	N-doped graphene hydrogel	2 Electrode configuration	2 mg ml^{-1} GO	5 M KOH	CC (10 A g^{-1})	190.1	95.2% (4000 cycles) (100 A g^{-1})	69 (2013)

Fig. 15 Schematic illustration for the formation of the HCGS sample. Reprinted (adapted) with permission from "high-performance supercapacitor electrodes based on highly corrugated graphene sheets, *Carbon*, 2012, **50**, 2179–2188" with permission from Elsevier.[62]

Another study looks at how the wrinkling in highly corrugated graphene sheets (HCGS) prevents aggregation of graphene sheets through their uneven surface area.[62] Such sheets are synthesized through thermal expansion and subsequent nitrogen cooling and these characteristics produce a BET area of 518 m^2 g^{-1}. The large BET area can be attributed to the curved surfaces of the graphene which prevents aggregation and these interesting morphological properties are a result of the thermal stresses experienced in the synthesis methodology. With the increase in effective surface area, a specific capacitance of 349 F g^{-1} was obtained in 6 M KOH electrolyte. The advantages of this method include a relatively simple synthesis method which results in a cheap, efficient and scalable process (Fig. 15).

Apart from increasing the effective surface area, there are also many other studies that aim to improve other factors that affect the supercapacitor performance as stated above. One such study illustrates how KOH treatment of graphene sheets led to an increase in edge effects and O_2 containing functional groups on the surface which resulted in an increase of 35% in capacitance.[63] However, such modifications come at a price as the BET area was reduced from 584 m^2 g^{-1} to 462 m^2 g^{-1} and this might have prevented achievement of highest possible capacitance. The authors explained the decrease through the blocking of pores *via* the introduction of functional groups on the surface.

Most recently, 3D graphene structures such as graphene gel as well as the doping of nitrogen onto graphene have been the focal point of much research as it was discovered that the addition of nitrogen atoms can positively improve the performance of graphene electrodes. In an investigation on such novel structures, a facile hydrothermal synthesis process was devised to produce nitrogen-doped graphene hydrogel (NGH) for supercapacitor applications. The hydrothermal synthesis

Fig. 16 Schematic showing KOH treatment of graphene to increase edge effects and O_2 containing functional groups.

process was selected amongst many other possible synthesis processes due to the relatively mild reaction conditions required as well as the advantage of scale up of the process. Organic amines such as ethylenediamine were used as the source of nitrogen for the doping process and could also alter the graphene 3D structure leading to improvements in performance. Results obtained from this study revealed that the graphene gel could achieve a high specific capacitance of 113.8 F g^{-1} and a power density of 205 kW kg^{-1} despite the extremely fast charge–discharge rate of 185 A g^{-1} and this allows it to be potentially used in devices that require high energy at fast rates.[69]

As illustrated in the preceding few paragraphs, most experiments were conducted with aqueous electrolytes such as KOH and Na_2SO_4 however, ionic liquids have gained popularity as alternative electrolytes of choice. Ionic electrolytes are known to have wide electrochemical windows of up to 4 V and their suitability in operating at high temperatures makes them ideal for electronic devices.[65] One such experiment involving both aqueous (H_2SO_4) and ionic electrolytes ($BMIMBF_4$) consists of the use of surfactants in graphene sheets to inhibit aggregation and improve surface wettability which leads to a higher specific capacitance. Surfactants such as tetrabutylammonium hydroxide (TBAOH), cetyltrimethylammonium bromide (CTAB) and sodium dodecylbenzene sulfonate (SDBS) were used and it was discovered that the highest capacitance of 194 F g^{-1} was obtained with TBAOH in H_2SO_4 (Fig. 16).

Lastly, extremely thin and transparent graphene films have been prepared for use in electronic equipment such as handphones due to an increasing demand for flexible and aesthetically pleasing electronics.[66] Such electrodes were prepared using vacuum filtration and produced 135 F g^{-1} with a width of 25 nm in 2 M KCl electrolyte.[67] A key incentive for producing such high quality transparent graphene films as electrodes is the high demand for these films in electronic devices such as handphones, laptop computers and mp3 players. Other advantages mentioned in the article include (1) excellent mechanical robustness of graphene which allows for flexible and strong graphene films that can be as thin as 25 nm. (2) The transparent nature of the films for use in transparent electronics. (3) The superior current capacity of graphene which allows for the omission of the charge–collector/electrode interface thus allowing electrodes to be simplified. (4) The solubility of graphene in many solvents meant that it could be used to be printed on different mediums and used in printable electronics (Fig. 17).

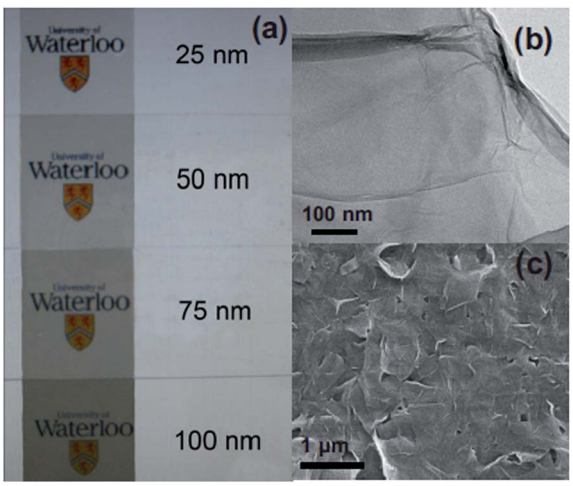

Fig. 17 (a) Photographs of transparent thin-films of different thickness on glass slides. (b) TEM image of graphene collected from dispersion before filtration. (c) SEM image of 100 nm graphene film on glass slide. Reprinted with permission from "ultrathin, transparent, and flexible graphene films for supercapacitor application, *Appl. Phys. Lett.*, **96**, 253105". Copyright [2010], American Institute of Physics.[67]

3.3 Graphene–polymer hybrids

Similar to the purpose of modifying graphene, for better supercapacitor electrodes, graphene–polymer composites play an important role in supercapacitor development. Electrically conducting polymers can by itself exhibit good specific capacitance due to the presence of a π electron conjugation system which enables fast and reversible redox reactions. However, limitations of using the polymer as a standalone material for electrodes include the fact that it is not as structurally robust as graphene and the durability of these materials is limited as a result of degradation from swelling and shrinkage of the polymer.[26] As such, it is shown in this section that a combination of graphene and electrically conducting polymers is beneficial. Not only would graphene provide good EDLC generation, the presence of polymers allows for faradaic reactions. However, unlike graphene modifications where the effective surface area was the most important factor in determining the capacitance, the importance of this factor is less clear in the case of graphene–polymer composites.[21] Instead, it is the interaction between graphene and polymers that is the significant factor in defining the capacitance. A variety of polymers such as polypyrrole (PPY), polyaniline (PANI), poly(3,4-ethylenedioxythiophene) (PEDOT), polythiophene (PT) and poly(*p*-phenylenevinylene) (PPV) were studied for supercapacitor components due to their ease of production and excellent capacitance. PANI, in particular, was investigated extensively compared to the rest of the polymers due to its promising electrochemical activity and thermal stability (Fig. 18).[26]

One such study involving carboxyl-functionalized graphene oxide (CFGO)–PANI composites was on the creation of CFGO–PANI composites through the *in situ* polymerization of PANI onto the basal oxygenated groups on graphene. This could only be done after the oxygenated groups were converted to carboxyl groups *via* chemical reactions. The authors believe that this would make the best use of these naturally occurring oxygenated groups on the basal plane as previous research studies have only made use of carboxyl groups at the edges to form PANI composites.[70] The resulting graphene–polymer composite showed a superior capacitance (525 F g^{-1}) at a current density of 0.3 A g^{-1} compared to previously synthesized graphene–polymer composites (323 F g^{-1}). This improvement in capacitance performance was attributed to the ability to bind more PANI chains as a result of the utilization of oxygen containing groups

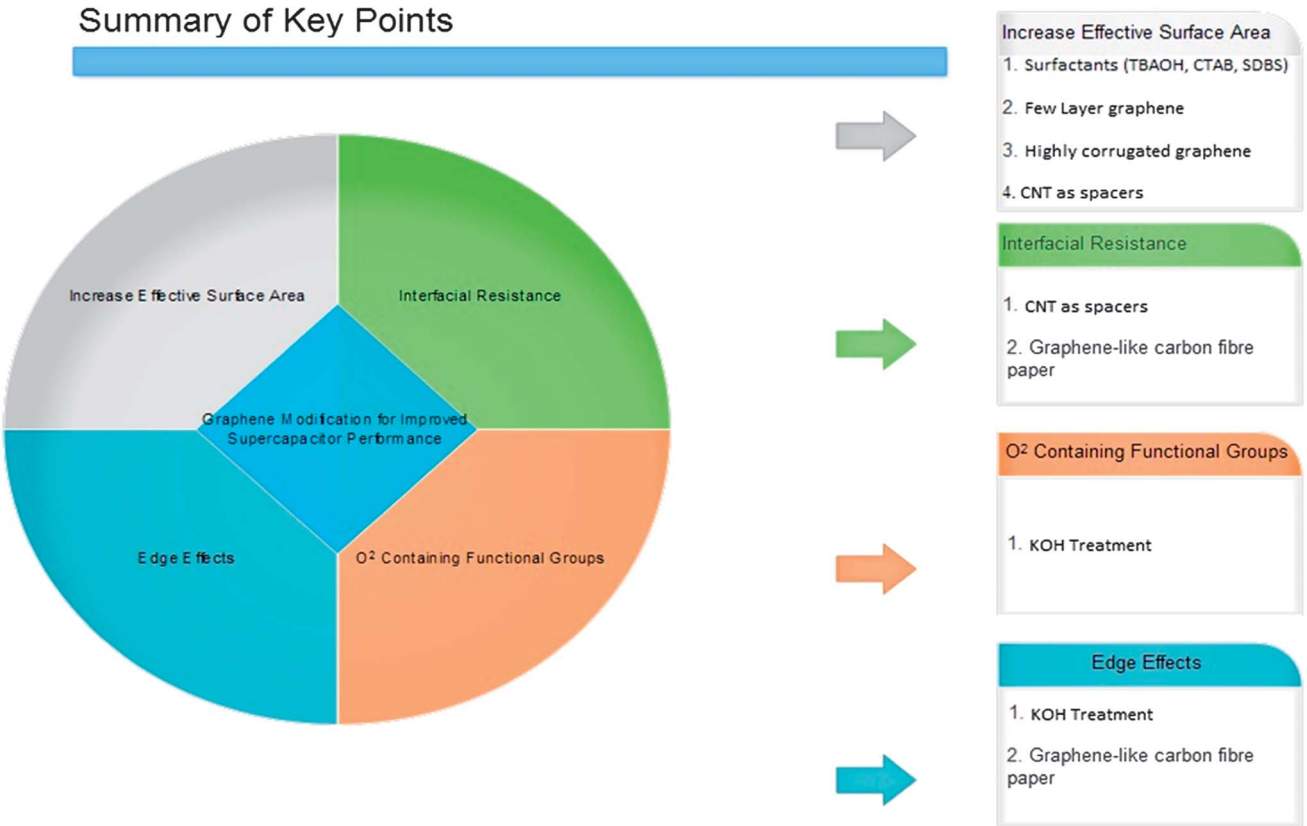

Fig. 18 Summary of key points for graphene modified supercapacitor.

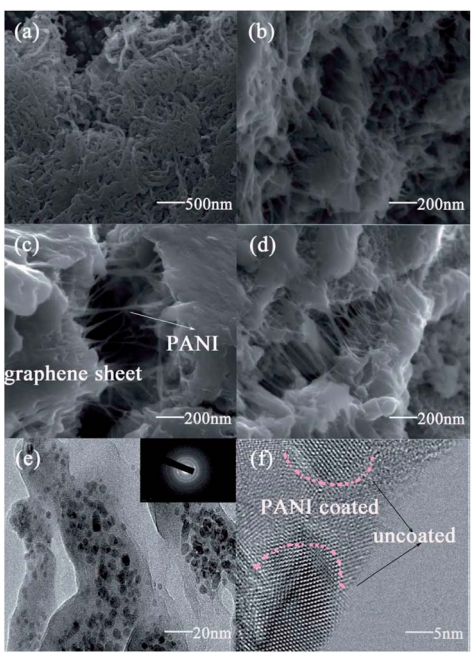

Fig. 19 SEM images of (a) PANI, (b) GO, (c) CFG–PANI and (d) CFGO–PANI. (e) TEM and (f) HRTEM of CFGO–PANI. The inset of (e) is the electron diffraction pattern of the CFGO–PANI composite. Reprinted (adapted) with permission from "carboxyl-functionalized graphene oxide–polyaniline composite as a promising supercapacitor material, *J. Mater. Chem.*, 2012, **22**, 13619". The Royal Society of Chemistry 2012 (ref. 70).

on the basal plane. One of the advantages of graphene–PANI composites is that the presence of graphene can improve PANI's electrical conductivity. In addition, such a composite can also improve the surface area of the electrode by preventing aggregation of graphene sheets through synergistic effects (Fig. 19).

A second study on graphene–PANI composites investigated how the introduction of certain molecules to graphene will lead to greater synergistic interactions between PANI and thus a higher capacitance. The study in particular concluded that the addition of amine groups (NH_2) led to an increase in capacitance and cycling stability and this corroborated with previous research studies that suggested that heteroatoms such as nitrogen compounds improved the capacitance.[69,71] Apart from the increase in capacitance after the addition of amine to the graphene–PANI composites, the capacitance also showed an increase (119%) despite undergoing 680 cycles and this is in contrast to other graphene–polymer composites that were tested. This is a very interesting study as it opens the possibility of adding amine groups to graphene and graphene composites such that they may make better electrodes in the future. Separately, the author also suggests that more studies should be conducted regarding graphene–PANI surface interactions and how PANI loading may affect the capacitance performance of such electrodes (Fig. 20).

Apart from the use of PANI for graphene–polymer composites, there has been research into other polymers for supercapacitor use. One such novel polymer that was rarely studied

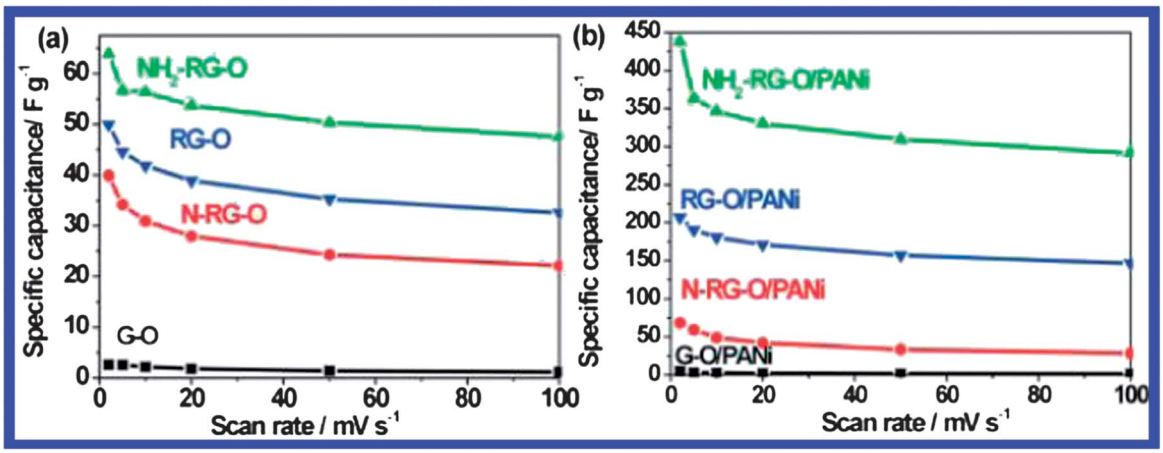

Fig. 20 Specific capacitance of different surface-functionalized graphene before (a) and after (b) loading of 10 wt% PANi asa function of scan rate (from 2 to 100 mV s^{-1}) in 1 M H_2SO_4 electrolyte. Reprinted (adapted) with permission from "preparation of supercapacitor electrodes through selection of graphene surface functionalities, Lai *et al.*, **6**(7), 5941–5951". Copyright (2012) American Chemical Society.[71]

was poly(*p*-phenylenediamine) (P*p*PD). Interest in PpPD arose as a result of the existence of additional free amino groups per monomer in the polymer chain as compared to PANI. In a study, PpPD and hydrogen exfoliated graphene have been synthesized *via* chemical oxidative polymerization in an acidic medium. The resulting material was studied for its specific capacitance and optimal polymer–graphene weight ratio. It was discovered that at a graphene to polymer weight ratio of 2 : 1, the highest supercapacitance of 248 F g^{-1} was obtained at a current density of 2 A g^{-1}.[26] However, the study did not hypothesize on the possible reasons as to why the weight ratios could significantly affect the capacitance and this could be an area of study in future research.[26]

Another interesting research that was carried out involved graphene–PPY composites. Although there has been much research in graphene and PPY as composites for electrodes, this research was unique as instead of using PPY fibres, PPY nanotubes were used as the composite material.[72,73] Such graphene–PPY nanotube composites have produced higher capacitance values (324 F g^{-1}) compared to the many previous investigations conducted on graphene–PPY fibre composites. The authors postulated that the superior capacitance was due to the nanotube structures which presented a greater surface area and macropore volume. This allowed the electrode to be exposed to more electrolytes and also facilitates ion transfer.[74]

Polyurethane (PU), which possesses shape memory properties, has also been combined with graphene to produce supercapacitor electrodes that can take on different shapes with both shape-retaining and shape-recovery abilities. Slightly similar to the transparent graphene films that were discussed in the "graphene modification" section above,[67] graphene–PU composites with their unique shape altering properties could satisfy the demand for flexible electrodes especially for non-conventionally shaped supercapacitors. In this study, graphene–PU composites were synthesized by a simple bonding method. Graphene was first produced *via* vacuum filtration from a GO/H_2O solution while PU was produced by casting from a PU/DMF solution. The PU film and graphene paper were then

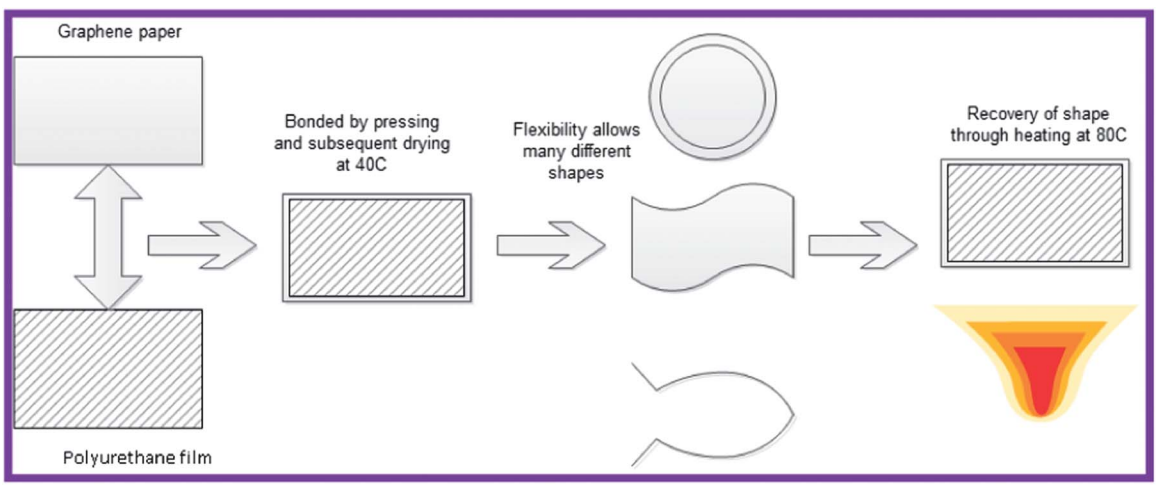

Fig. 21 Diagram showing graphene–PU composite and its properties.

bonded by pressing and subsequent drying at 40 °C. This novel composite makes use of the flexibility of graphene and the assistance of PU to ensure that shape controllable electrodes could be created thus meeting the increasing demand of such electrode types in today's world. PU is part of a class of materials known as shape-memory polymers. This class of materials have shape altering properties that are dependent on the temperature. In the PU case, the shape of PU can be fixed at room temperature and recovered by heating it to 80 °C. In addition to their useful shape-changing properties, these graphene–PU electrodes can achieve a maximum capacitance of 218 F g^{-1} at a current density of 0.5 A g^{-1}. Good durability and cycling ability were also demonstrated as the electrode maintained 95% of its capacitance performance after 2000 cycles. The high capacitance was attributed to the superior EDLC and electron transport properties of graphene while the excellent stability was credited to the stable structure of the graphene–PU composite (Fig. 21).[75]

Apart from studies conducted on the types of polymers used for these graphene composites, it is generally useful to investigate the architecture of these graphene–polymer composites to determine the most effective configuration for such electrodes. One such study identified how graphene oxide (GO) sheets could be layered with polymers in between to encourage superior capacitance performance.[76] Such an approach is based on the principles of electrostatic interactions between the positively charged surfactants and negatively charged GO sheets. These surfactants are first introduced into the interlayer of the graphene sheets where they form a layered GO-surfactant micelle structure. Polymer monomers are then introduced and they would solubilize in the hydrophobic cores of the micelles. Polymerization then occurs through the help of an initiator and the structure is eventually washed to remove the surfactant molecules thus leaving the GO–polymer composite. A follow up investigation revealed that such GO–polymer structures produced electrodes with superior capacitance compared to commercial ones. The GO–PPY composite produced *via* this method exhibited a capacitance of 510 F g^{-1} at a current density of 0.3 A g^{-1} in 2 M H_2SO_4 and this was greater than the value of 400 F g^{-1} achieved under similar conditions for the graphene–PPY nanotubes in a study discussed above.[74] The advantages of using this novel structure for future graphene–polymer composites are as follows. (1) The exfoliated GO sheets in the solution will provide an extensive surface area for polymers to attach on both sides of the surface. (2) The 3D layered structure of the composite would increase the mechanical robustness of the electrode and also acts as a stabilising factor for the polymer. (3) This novel structure can reduce the resistance towards the electrolytes. (4) The presence of the polymers will allow pseudocapacitance and faradaic reactions thus increasing the capacitive performance (Fig. 22).

3.4 Graphene–metal oxide supercapacitors

Graphene–metal oxide composites have been rigorously studied in recent years as they present a unique proposition to enhance

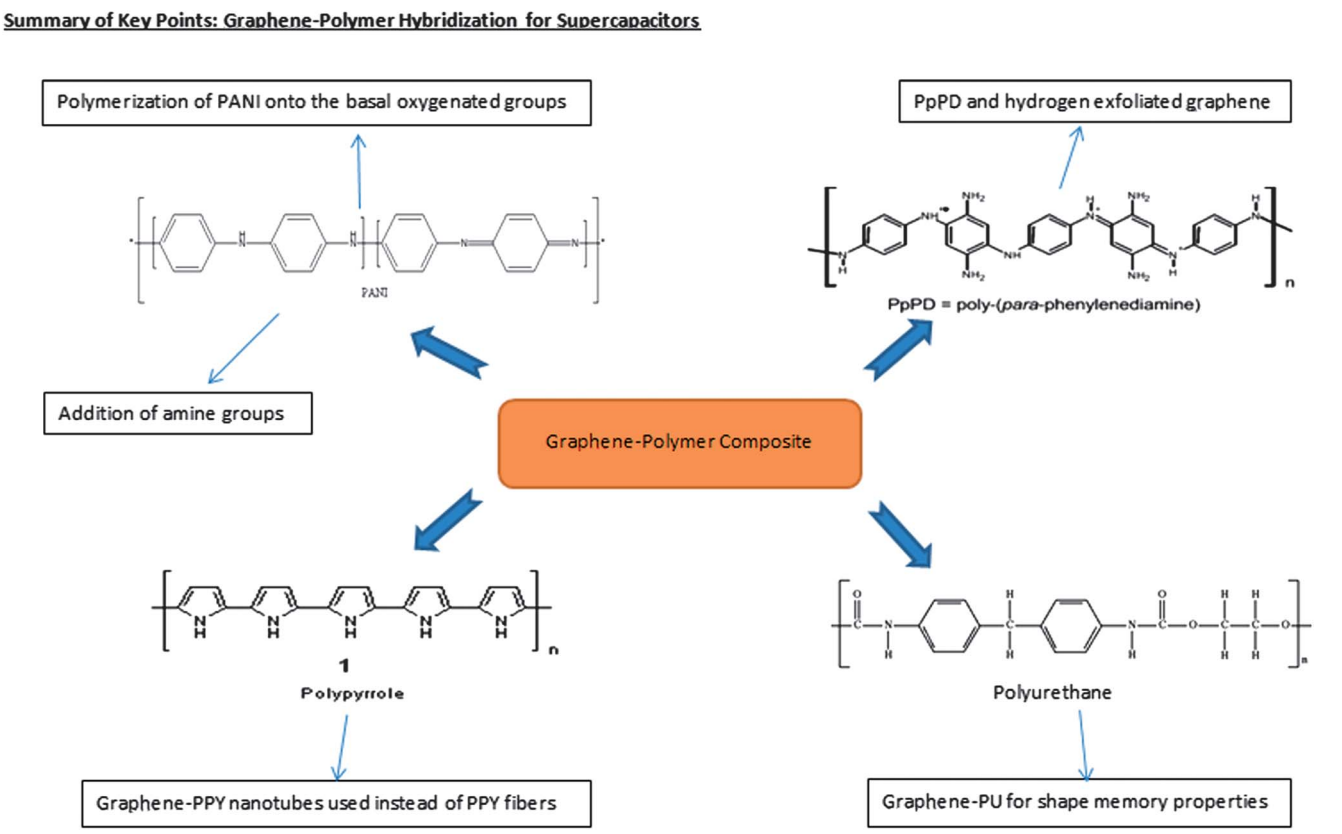

Fig. 22 Summary of key points for graphene–polymer hybridization for supercapacitors.

Table 3 Summary of research results for graphene–polymer hybrid supercapacitors

Preparation method	Nature of electrode	Electrode configuration	Mass/SA of electroactive materials	Electrolyte	Measurement protocol	Maximum capacitance ($F\ g^{-1}$)	Capacitance retention	Ref. (year)
In situ polymerization	Graphene oxide–polyaniline	3 Electrode configuration	3 mg	1 M H_2SO_4	CV (ν = 10 mV s^{-1}) (0.3 A g^{-1})	525	91% (200 cycles)	70 (2012)
Ultrasonication and filtration	Layered graphene with polymers	3 Electrode configuration	1 mg cm^{-2}	2 M H_2SO_4	CV (ν = 50–400 mV s^{-1}) (0.3 A g^{-1})	510	70% (1000 cycles)	76 (2010)
Chemical oxidation polymerization	Poly(*p*-phenylenediamine) and H_2 exfoliated graphene	2 Electrode configuration	Weight ratio of polymer to graphene varies	1 M H_2SO_4	CV (ν = 10 mV s^{-1}) (2 A g^{-1})	248	72% (1000 cycles)	26 (2012)
In situ polymerization	Graphene oxide-polyaniline	3 Electrode configuration	2–3mg (320 $m^2\ g^{-1}$)	0.5 M H_2SO_4	CV (ν = 2 mV s^{-1}) (1–1.5 A g^{-1})	500	119% (680 cycles)	71 (2012)
Simple bonding method	Graphene–polyurethane	3 Electrode configuration	—	1 M H_2SO_4	CV (0.5 A g^{-1})	218	95% (2000 cycles)	75 (2012)
Ultrasonication	Graphene–polypyrrole	3 Electrode configuration	—	2 M H_2SO_4	CV (ν = 2–5mV s^{-1}) (0.3 A g^{-1})	400	88% (200 cycles)	74 (2012)
In situ polymerization	Graphene–polyaniline	3 Electrode configuration	2–3 mg active material	3 M KOH	CV (ν = 1 mV s^{-1})	463	90.6% (500 cycles)	77 (2013)

the electrode performance in supercapacitors. Similar to graphene–polymer composites, these metal composites allow electrodes to achieve both high EDLC, through the graphene, and pseudocapacitance, through the metal oxides. The increased effectiveness of such composites can be best observed by comparing the capacitance obtained by pure graphene *versus* that by metal oxide composites. Pure graphene electrodes have been known to achieve an EDLC of 135 F g^{-1}.[78] On the other hand, graphene–metal oxide composites can easily achieve capacitance values as high as 135 F g^{-1} (refer to Table 3 for comparison between performances of different graphene–metal oxide composites). Other advantages of graphene–metal oxide composites include the fact that standalone metal oxide composites exhibit weak electrical conductivities thus leading to poor cycling and capacitance performance. In addition, graphene–metal oxide composites reduce the need for binders thus eliminating possible aggregation of nanostructures and side reactions.[79] It is also important to note that parameters such as polymorphism, morphology, particle size, and bulk density will affect the electrochemical properties of metal oxides such as MnO_2.[80] In this section, various graphene–metal oxide composites (Mn, Co, Ni, Ti, Ru) and their respective performances and limitations will be discussed.

One of the most extensively studied metal oxides for supercapacitor applications is RuO_2 due to its high capacitance performance. In a recent study, amorphous hydrous RuO_2 nanoparticles on H_2 exfoliated graphene have been hydrothermally synthesized and tested for their electrochemical performance.[81] RuO_2 was chosen due to its superior pseudocapacitance and cycling ability thus making it an excellent electrode material for supercapacitor applications.[82] The hydrothermal synthesis methodology used ensures that the RuO_2 particles are well dispersed onto the graphene sheets and this allowed the electrode to achieve a specific capacitance of 154 F g^{-1} and an energy density of 11 W h kg^{-1} at a current density of 1 A g^{-1} in 1 M H_2SO_4 solution.[81] Further improvements such as the deposition of RuO_2 onto functionalized graphene sheets could help improve the specific capacitance. In addition, this method of synthesizing well dispersed graphene–RuO_2 composites could be used with many other metal oxides as alternatives (Table 4).[81]

However, RuO_2 is both costly and toxic thus recent studies have largely shifted to cheaper alternative metal oxides such as nickel oxide, cobalt oxide and manganese oxide. Mn_3O_4 is largely preferred as Ni and Co composites are limited to only alkaline electrolytes which have a small potential window (0.4–0.5 V). Since the energy density is proportional to the cell voltage, therefore, electrolytes with small potential windows will limit the energy density and specific capacitance.[83] Mn_3O_4, on the other hand, has been increasingly popular because it is cheap, and show environmental compatibility and intrinsically high capacity.[83,84] In one recent study Mn_3O_4 nanorods were synthesized on graphene sheets *via* a hydrothermal synthesis approach. This approach used ethylene glycol as a reducing agent and is similar to the synthesis method for RuO_2 that was discussed above.[81] As such, a good dispersion of nanoparticles on the graphene surface was achieved and the final material

Table 4 Summary of research results for graphene–metal oxide hybrid supercapacitors

Preparation method	Nature of electrode	Electrode configuration	Mass/SA of electroactive materials	Electrolyte	Measurement protocol	Maximum capacitance (F g^{-1})	Capacitance retention	Ref. (year)
Hydrothermal process	Graphene–Mn_3O_4	3 Electrode configuration	2 mg	1 M Na_2SO_4	CV (ν = 50 mV s^{-1}), (0.5 A g^{-1})	121 F g^{-1}	100% (10 000 cycles)	83 (2012)
2-Step coating process	Graphene–Mn_3O_4 with conductive wrapping	3 Electrode configuration	~0.1 mg cm^{-2}	0.5 M Na_2SO_4	CV (ν = 100 mV s^{-1})	380 F g^{-1}	95% (3000 cycles)	93 (2011)
2-Step surfactant method	Graphene–Co_3O_4 scrolls	3 Electrode configuration	—	6 M KOH	CV (ν = 5 mV s^{-1}), (1 A g^{-1})	159.8 F g^{-1}	93% (1000 cycles)	87 (2011)
Self-limiting deposition	Graphene–Mn_3O_4	3 Electrode configuration	3 mg (64% wt of MnO_2)	1 M Na_2SO_4	CV (ν = 2 mV s^{-1})	310 F g^{-1}	95.4% (15 000 cycles)	85 (2010)
Electrophoretic deposition and chemical reduction	GO/Co_3O_4/MnO_2	3 Electrode configuration	—	1 M KOH	CV (ν = 100 mV s^{-1})	117 F g^{-1}	—	79 (2012)
Electrophorectic and chemical-bath deposition	Graphene–NiO hybrid film	3 Electrode configuration	1.25 mg cm^{-2}	1 M KOH	CV (ν = 10 mV s^{-1}), (2 A g^{-1})	400 F g^{-1}	94% (2000 cycles)	88 (2011)
Hydrothermal synthesis	$RuO_2 \cdot xH_2O$/HEG	2 Electrode configuration	20% wt Ru	1 M H_2SO_4	CC (1 A g^{-1})	155 F g^{-1}	—	81 (2011)
Electrostatic interaction	MnO_2/CNT/graphene	3 Electrode configuration	4 mg, 37% wt RGO	1 M Na_2SO_4	CC (0.2 A g^{-1})	193 F g^{-1}	70% (1300 cycles)	86 (2012)
—	TiO_2/rGO/NB	2 Electrode configuration	20.9 m_2 g^{-1}	1 M Na_2SO_4	CV (2 mV s^{-1})	200 F g^{-1}	91.1% (200 cycles)	89 (2012)
Mild hydrothermal	GNS/MnO_2	3 Electrode configuration	—	1 M Na_2SO_4	CC (5 mA cm^{-2})	263 F g^{-1}	99% (500 cycles)	80 (2012)
Hydrothermal process	$MnCO_3$/graphene hydrogel	3 Electrode configuration	0.4 $MnCO_3$: 1 GO	6 M KOH	CC (0.5 A g^{-1})	645.5 F g^{-1}	—	94 (2013)

showed a specific capacitance of 121 F g^{-1} and retained 100% of that capacitance after 10 000 cycles.[83] This was 3–4 times higher than the specific capacitance obtained for pure Mn_3O_4 electrodes.[83] The reason for the better performance is due to the fact that pure Mn_3O_4 electrodes have poorer conductivities and also the synthesis method mentioned above allows good dispersion of nanorods thus increasing the accessibility of electrolytes to the composite and also preventing aggregation.

Another recent study on graphene–MnO_2 composites reported an extremely high specific capacitance of 310 F g^{-1} at a scan rate of 2 mV s^{-1}.[85] This performance is about 3 times greater than that of pure graphene as well as birnessite-type MnO_2. This graphene–MnO_2 composite was synthesized *via* self-limited deposition of MnO_2 on the graphene surface under microwave irradiation. The drastic improvement in performance was attributed to the extensive graphene surface to deposit MnO_2 particles thus increasing the electrical conductivity and increasing the interaction area between MnO_2 and graphene and electrolyte.[85] The author further adds that the performance achieved by this composite is the best amongst all known MnO_2–carbon composites at the time of publication and is optimistic that this relatively simple, cheap and environmentally friendly way of synthesizing such composites will encourage their application in future electrochemical systems.

Meanwhile, in an investigation conducted by Lei and co-workers MnO_2 was introduced onto a graphene–CNT structure to create a graphene–MnO_2 composite that could be used for electrodes in supercapacitors.[86] This graphene–CNT structure is similar to the one discussed in the 'graphene modification' section above where CNTs were used as spacers and binders to prevent the aggregation of graphene sheets while simultaneously holding the graphene sheets together.[55] However in this case, MnO_2 was first added to the CNT before poly(diallyldimethylammonium chloride) (PDDA) was used to functionalise the MnO_2/CNT structure to give it the positive charge needed to electrostatically attract the graphene sheets which were negatively charged. The resulting composite showed a specific capacitance of 193 F g^{-1} and retained 70% of its capacitance after 1300 cycles when 37% reduced graphene oxide was used.[86] The percentage of graphene oxide used affects performance capabilities and should thus be controlled. For example, when 54% of reduced graphene oxide was used, graphene sheets started to aggregate and the authors postulated that this was due to insufficient spacers from the lack of MnO_2/CNT.[86]

3D urchin-like MnO_2–graphene composites have also been studied for their suitability for application as supercapacitor electrodes. These unique MnO_2 nanoparticles are grown on the graphene sheets directly and act as spacers to prevent aggregation of adjacent graphene sheets. The synthesis of these composites as well as mild hydrothermal methods involved the deposition of MnO_2 onto the graphene sheets. The unique composite structure allows an increased rate of interaction between the electrolyte and the electrodes and accounts for a high specific capacitance of 263 F g^{-1} and a long cycle life.[80]

While MnO_2 composites are the most common type of manganese composite used for graphene-based electrodes, $MnCO_3$ composites have also been studied and proved to be suitable alternatives. $MnCo_3$ was chosen as a material for study because it is cheap and abundant. In this study, graphene–$MnCO_3$ hydrogel (GMH) composites were hydrothermally synthesized and a maximum capacitance of 613.8 F g^{-1} was obtained under a discharge current of 0.7 A g^{-1} in a three-electrode system. The study noted that a specific capacitance of 173.8 F g^{-1} was obtained under the same conditions in a two-electrode system and the reason for the difference was the presence of an extra electrode in the three-electrode system. Further reasons for this difference in the obtained results are discussed in the "Best Methodology for Electrode Performance Test" section of this report. The study also investigated how the addition of different amounts of $MnCl_2$ led to different performance values and concluded that excess or minimal loading of $MnCl_2$ will result in the formation of the GMH composites thus reducing capacitance performances. It concluded that the optimal weight ratio of $MnCl_2$ to GO is 0.4 : 1.[94]

Apart from Mn oxide composites, other graphene–metal oxide composites have also been explored for electrodes in supercapacitor applications. A novel scroll-like structure of the graphene–Co_3O_4 composite has been synthesized *via* a simple 2-step method with the assistance of sodium dodecyl sulfate (SDS).[87] Unlike many other composites where the metal oxide particles are intercalated onto the graphene sheets, in this

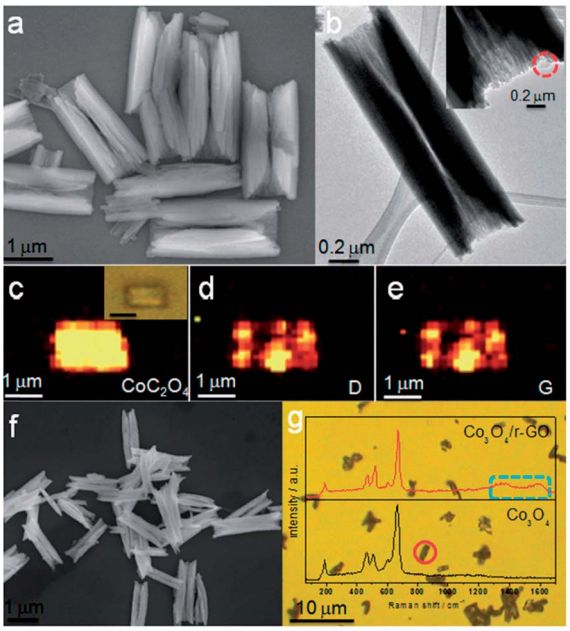

Fig. 23 (a) SEM image of the CoC_2O_4–GO scrolls. (b) TEM image of a single CoC_2O_4–GO scroll. (c–e) Raman mapping images of CoC_2O_4 and D, G bands of GO for a single CoC_2O_4–GO scroll; inset in (c) shows the optical image of the selected CoC_2O_4–GO scroll. The scale bar of the inset is 1 mm. (f) SEM image of the Co_3O_4–r-GO scrolls. (g) Optical image of the Co_3O_4–r-GO scrolls and Raman spectra of pure Co_3O_4 (for reference) and Co_3O_4–r-GO obtained from a single scroll marked by a red circle in the optical image. The Raman signals of r-GO are highlighted with a blue dashed rectangular box. Reprinted (adapted) with permission from "fabrication of Co_3O_4–reduced graphene oxide scrolls for high-performance supercapacitor electrodes, *Phys. Chem. Chem. Phys.*, 2011, **13**, 14462–14465" PCCP.[87]

method reduced graphene platelets are intercalated instead into the Co_3O_4 scrolls. This integration was achieved through the interaction between Co_3O_4 and the oxygen functional groups on the reduced graphene oxide. The resulting reduced graphene oxide–Co_3O_4 composite attained a specific capacitance of 168 F g^{-1} at a discharge current of 1 A g^{-1} and the authors postulated that the good electrode performance was due to the unique structure and synergistic effects between graphene and Co_3O_4 (Fig. 23).[87]

Graphene–NiO hybrid films have also been studied and a pseudocapacitance of 400 F g^{-1} was achieved at a discharge current of 2 A g^{-1}. This composite film was synthesized by electrophoretic deposition (EPD) and chemical bath deposition (CBD). The improved pseudocapacitance performance was attributed to the incorporation of graphene which greatly increases the rate of oxidation of Ni^{II} to Ni^{III} and this increased electrochemical activity led to faster faradaic reactions and thus higher pseudocapacitance.[88]

Besides studies on the different graphene–metal oxide composites, important research studies into the effects of metal oxide structures and their interactions with graphene were also reported. In a recent study, the performance of electrodes made out of reduced graphene oxide (rGO)–TiO_2 nanobelts (NB) was compared with rGO–TiO_2 nanoparticles (NP). It was discovered that rGO–TiO_2 nanobelts performed much better than the rGO–TiO_2 nanoparticles by a factor of almost 4 (225 F g^{-1} to 62.8F g^{-1}).[89] This was due to the point and planar interactions of the nanoparticles and nanobelts with respect to rGO. It was obvious that the planar interactions between rGO and nanobelts would create a larger contact area thus enhancing the transfer area between the two materials for better electrode performance. This largely corroborated with other studies which suggests that 1D nanostructures showed superior electrode performance compared to zero dimensional particles.[90–92] In addition to the investigation on how metal oxide structures influence the electrode performance of these graphene–TiO_2 composites, the mass loading ratio of these composites was also studied. It was discovered that the optimal mass loading for graphene–TiO_2 composites was 7 : 3.[89] When too much TiO_2 was added, aggregation occurred and defect sites appeared on the graphene thus leading to a poorer electrode performance. However, when too little TiO_2 was added, the area of contact between metal oxide and graphene was not optimized. Further research into mass loading ratios and metal oxide structures and their coupling effects with graphene could provide more clues into the optimal graphene–metal oxide composite configuration for supercapacitor applications (Fig. 24 and 25).

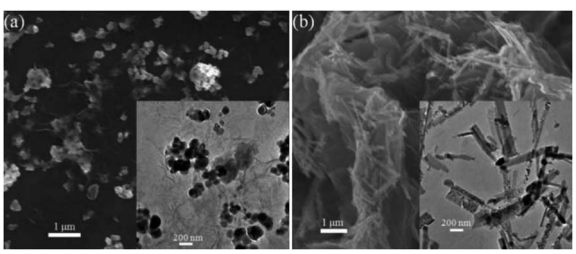

Fig. 24 SEM images of rGO–TiO_2 NPs (a) and rGO–TiO_2 NBs (b) with a rGO : TiO_2 ratio of 7 : 3. Insets: TEM images. Reprinted (adapted) with permission from "reduced graphene oxide–titanium dioxide composites for supercapacitor electrodes: shape and coupling effects". The Royal Society of Chemistry 2012.[89]

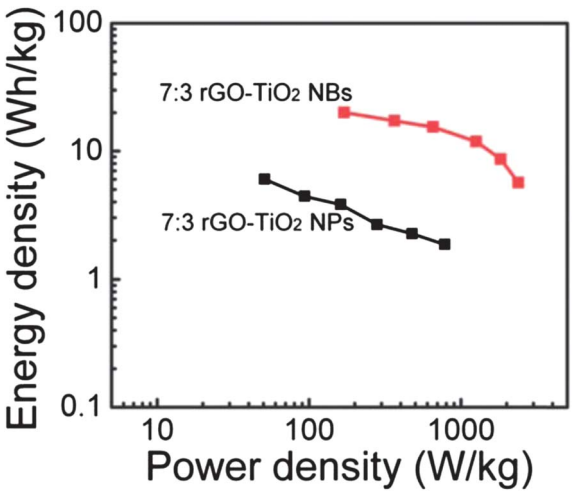

Fig. 25 Ragone plots of the rGO–TiO_2 NPs and the rGO–TiO_2 NBs at 7 : 3 mass ratio at different current densities. Reprinted (adapted) with permission from "reduced graphene oxide–titanium dioxide composites for supercapacitor electrodes: shape and coupling effects". The Royal Society of Chemistry 2012.[89]

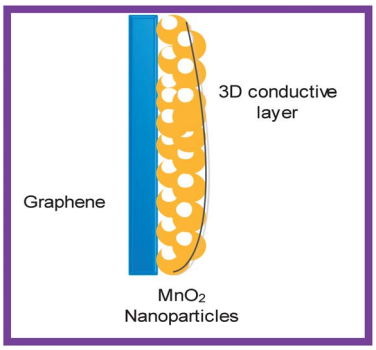

Fig. 26 Schematic of conductive layer approach.

An interesting study was also conducted using hybrid metal oxide nanostructures instead of the usual single metal oxide nanostructure to form graphene–metal oxide composites. This unique hybrid composite was designed by coating Co_3O_4 nanowires onto MnO_2 nanostructures.[79] The synergistic effects of these two metal oxides were rather significant as a little MnO_2 added to Co_3O_4 could increase the specific capacitance by a large value. rGO was further added on top of the MnO_2–Co_3O_4 hybrid composite *via* electrophoretic deposition and chemical reduction to allow EDLC as well as efficient contact with electrolytes. This unique hybrid graphene–metal oxide composite opens the door to extensive research on the synergistic effects between these components and possibly other permutations of hybrid metal oxide composites.

Lastly, a type of 3D conductive layer approach has been used to drastically increase the specific capacitance of graphene–metal oxide composites (Fig. 26). One of the major limitations

for graphene–MnO_2 electrodes as well as other graphene–metal oxide electrodes is the need for high mass loading especially when developing electrodes for devices that require high energy densities. A high mass loading of the metal oxide however would typically increase the electrode resistance due to the high density packing of the metal oxide which reduces the effective surface area for pseudocapacitance. In this study, the authors have developed a 3D conductive layer wrapping that aims to reduce this limitation. Graphene–MnO_2 composites were used in this investigation and it was discovered that this conductive layer approach increased the specific capacitance by as much as 45% with capacitance values peaking at 380 F g^{-1}. In addition, such composites also displayed excellent cycling stability with 95% retention in capacitance over 3000 cycles. The conductive layer can be made with either carbon nanotubes (CNT) or conductive polymers and their purpose is to create an additional layer in which pseudocapacitance can take place as well as provide another alternative electron transport pathway.[93]

3.5 Asymmetric supercapacitors

In the previous sections, symmetric supercapacitors were often used to test the specific capacitance of graphene based electrodes. However, asymmetric supercapacitors, where two different electrodes are used instead of the same type, have attracted increasing attention as they have been shown to be capable of attaining higher energy densities while maintaining their power densities.[95] This is achieved by using different types of materials as electrodes that work in different electrochemical potential window ranges within the same aqueous electrolyte. This would thus broaden the cell voltage of the aqueous electrolyte and increase the energy density. Notably, supercapacitors based on ionic or organic electrolytes have much higher electrochemical potential windows and could thus achieve energy densities of around 80 W h kg^{-1}. However, ionic liquids are known to be rather expensive and organic electrolytes have their own downsides such as poor electric conductivity and as such may not be as desirable in all practical applications (Table 5).[96]

At present, the most widely used types of asymmetric capacitors are activated carbon types. Activated carbon is chosen due to its extensive surface area and relatively low cost. However, disadvantages of using activated carbon include the small porous surface (0.5 nm) which prevents the entry of hydrate ions which typically range in sizes of 0.6–0.76 nm.[97] Instead, graphene is now being considered as a better material for asymmetric supercapacitors due to its flexible pore structure, excellent conductivity and mechanical properties as well as high stability and extensive surface area. As such, hydrate ions can be transported at high rates which will facilitate the formation of excellent EDLC in aqueous electrolytes.[97]

A study to show how asymmetric supercapacitors could produce higher energy densities compared to symmetric supercapacitors was conducted by Zhang and co-workers.[96] In this study, an asymmetric supercapacitor with reduced graphene oxide (RGO) and ruthenium oxide was fabricated as the anode while the RGO–PANI electrode was fabricated as the

Table 5 Summary of research results for graphene aymmetric supercapacitors

Preparation method	Cathode (−)	Anode (+)	Energy density	Power density	Electrolyte	Maximum capacitance (F g^{-1})	Capacitance retention	Ref. (year)
RGO sheets with sonication of $RuCl_3$	RGO–PANi	RGO–RuO_2	26.3 W h kg^{-1}	49.8 kW kg^{-1} at 6.8 W h kg^{-1}	2 M H_2SO_4	357 F g^{-1} at 0.3 A g^{-1}	80% after 1000 cycles and 70% after 2500 cycles	96 (2011)
Microwave assisted method	Porous graphene	$Ni(OH)_2$/graphene	77.8 W h kg^{-1}	174.7 W kg^{-1}	6 M KOH electrolyte	218.4 F g^{-1}	94.3% after 3000 cycles	98 (2012)
Redox reaction under microwave irradiation	Activated carbon nanofibers	Graphene/MnO_2	51.1 W h kg^{-1}	198 kW kg^{-1}	1 M Na_2SO_4	113.5 F g^{-1} at 1 mV s^{-1}	97% after 1000 cycles	99 (2011)
Reduction, intercalation and exfoliation	Graphene	MnO_2 nanowire/graphene	30.4 W h kg^{-1}	5000 W kg^{-1} at 7.0 W h kg^{-1}	1 M Na_2SO_4	31.0 F g^{-1}	79% after 1000 cycles	97 (2010)
Electrophoretic deposition	Electrophoretic graphene	MDANF	<65.9 W h kg^{-1}	<180 W kg^{-1}	0.5 M Na_2SO_4	132.6	30.6% after 1000 cycles	100 (2013)
Coating	Activated carbon	MDANF	65.9 W h kg^{-1}	180 W kg^{-1}	0.5 M Na_2SO_4	146.5	27% after 1000 cycles	100 (2013)

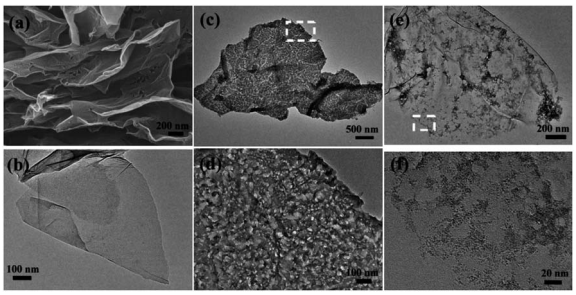

Fig. 27 FESEM image of a RGO sample prepared using a microwave-assisted reduction method (a). TEM images of RGO (b), RGO–PANi (c and d), and RGO–RuO_2 (e and f).[96] Reprinted (adapted) with permission from "A high-performance asymmetric supercapacitor fabricated with graphene-based electrodes". The Royal Society of Chemistry 2011.

cathode. The attained energy density of this asymmetric supercapacitor (26.3 W h kg^{-1}) was compared to a symmetric RGO–RuO_2 capacitor (12.4 W h kg^{-1}) and a RGO–PANI capacitor (13.9 W h kg^{-1}) and was found to be around 2 times higher than the energy densities achieved by these symmetric supercapacitors.[96] In addition, the asymmetric capacitor exhibits cycling stability with a retention ratio of 80% after 1000 cycles and 70% after 2000 cycles. It also achieved a remarkable power density of 49.8 kW kg^{-1} at an energy density of 6.8 W h kg^{-1} (Fig. 27).

Yan and co-workers studied how flower-like nickel hydroxide–graphene can be used as a positive electrode and porous graphene as a negative electrode in an asymmetric capacitor. The flower-like graphene composites were prepared *via* a microwave heating approach and templates or precipitate controlling agents are unnecessary. This flower-like structure was chosen over other morphological structures, such as microspheres, nanotubes and platelet like structures, due to its shorter diffusion path length for ions and electrons in the electrolytes thus allowing rapid charge and discharge

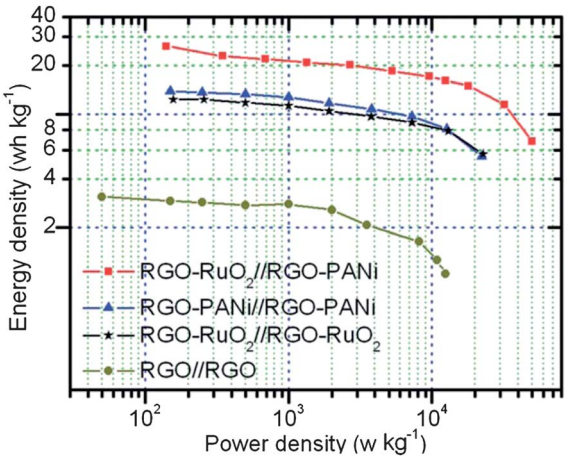

Fig. 28 Ragone plots of symmetric and asymmetric supercapacitors based on RGO, RGO–RuO_2, and RGO–PANi.[96] Reprinted (adapted) with permission from "a high-performance asymmetric supercapacitor fabricated with graphene-based electrodes". The Royal Society of Chemistry 2011.

processes.[98] The asymmetric capacitor showed an electrochemical potential window of 0 to 1.6 V and displayed a specific capacitance of 218.4 F g^{-1} as well as an energy density of 77.8 W h kg^{-1}. In addition, this device also showed long stable cycling ability with 94% retention in capacitance after 3000 cycles.[98] The authors ascribe these superior performances to the excellent synergistic effects of the 2 electrodes (Fig. 28).

Other graphene–metal oxide composites such as graphene–MnO_2 have also been chosen as positive electrodes for asymmetrical capacitors. Such composites make good positive electrodes as their small nanoparticle size and excellent electroconductivity allow fast faradaic reactions to take place at high power densities. In addition, materials with extensive surface area and good electric conductivity, such as activated carbon, should be used as negative electrodes so as to produce many double layers which would allow efficient transportation of electrolyte ions and thus good energy and power densities. One such study uses the above configurations to test for electrode performance and the electrode obtained an energy density of 51.1 W h kg^{-1} with excellent cycling stability and a retention capacity of 97% after 1000 cycles.[99]

As MnO_2 is one of the most promising and popular metal oxides used in capacitors, many research studies on asymmetric capacitors also involves the use of this material. Another such study on graphene–MnO_2 nanowire composites in Na_2SO_4 electrolytes involved the use of graphene as the negative electrode and the MnO_2–graphene composite as the positive electrode. This composite was fabricated *via* a solution-phase assembly technique and CV and galvanostatic charge–discharge measurements showed that the electrochemical potential window has been increased to 2 V. The authors attributed this increase to the synergistic combination of the positive and negative stabilities of the 2 different electrodes at different potential windows. The maximum measured energy density obtained for this configuration is 30.4 W h kg^{-1}, which is higher than the case when symmetric graphene (2.8 W h kg^{-1}) or symmetric graphene–MnO_2 nanowire composite electrodes (5.2 W h kg^{-1}) were used. In addition, a cycling performance with 79% of initial capacitance was obtained after 1000 cycles thus promising good stability. The authors believe that further research into the optimum mass/volume ratio of electrodes, weight ratios of graphene in the graphene–MnO_2 nanowire composite electrodes as well as the structures of both graphene and MnO_2 could lead to significant improvements in the performance of these capacitors.[97]

Very recently, a study conducted by Tang and co-workers delved into the impacts of negative and positive electrode characteristics in achieving superior capacitance in asymmetric capacitors.[100] The study used manganese dioxide, Au, and nickel form (MDANF) composite as the positive electrode and either graphene or activated carbon (AC) as the negative electrode. The electrodes were immersed in 0.5 M Na_2SO_4 solution and several tests were carried out. To study how the differing mass ratios of electrodes could affect the capacitor performance, an active material quantity of 1 mg was used for the positive electrode (MDANF) while the active material for graphene and AC was varied in ranges of 1.25 to 3.1 mg and 1.01 to 2.88 mg

respectively. It was discovered that the optimum mass ratios that would demonstrate rectangular CV curves are $(m_{graphene(-)}/m_{(+)}) = 1.84$ and $(m_{Ac(-)}/m_{(+)}) = 1.75$ respectively. This however differed from the theoretically calculated mass ratios of 2.6 and 2.2 for graphene and AC respectively and the reason postulated was the underestimation and overestimation of the negative and positive electrode's shared potential window respectively. These findings highlighted the importance of electrode mass ratios in determining capacitance values in supercapacitors.[100]

The second finding in the study illustrated how the composition of the negative electrode could affect both specific capacitance and power performances in a supercapacitor. An analysis of AC asymmetric capacitors revealed that it has a better rate capability as compared to graphene type capacitors due to its ability to operate at high scan rates of 300–500 mV s^{-1}. The study also showed that AC asymmetric capacitors have superior capacitance performance compared with graphene type asymmetric capacitors (146.5 F g^{-1} *vs.* 132.6 F g^{-1}). Lastly, it was found that different types of negative electrodes, such as AC or graphene, have little impact on the stability of the supercapacitor performance.[100]

4 Best methodology for electrode performance testing

As described in the previous sections, the key factor that reflects the performance of supercapacitors is the capacity of the electrodes to store and release energy. This, in turn, is often determined by the electrode material. This justifies the numerous research studies over the years on the use of different types of materials for the formation of electrodes, with graphene-based electrodes gaining much popularity. It is well known that the best test for electrode performance would be to use it in a full-scale commercial application scenario. Obviously, such testing methods result in many limitations as it is simply not cost and time-effective to design full-scale cells for all tests. Therefore, the goal of this section is to review all test-cell configurations and measurement methods that have been used in the field of electrode testing and try to find the optimal configuration and measurement method that would allow accurate, repeatable testing of electrode performance.

4.1 Test-cell configuration

As shown in the summary of test results in the earlier sections of this report, the test-cell configuration for electrode performance testing typically consists of either 2 or 3 electrodes. These two different test-cell configurations will yield distinctively different results and should only be used to test electrodes in the appropriate setting.

A typical 3 electrode cell consists of a reference electrode, a working electrode and a counter electrode. Only the working electrode would contain the material that is being tested for its electrochemical properties. In addition, the voltage potential applied to the working electrode is highly dependent on the reference electrode and would normally yield 2 times more capacitance compared to a 2-cell electrode configuration.[101] As a result, these attributes make the 3-cell electrode configuration especially sensitive and this could result in significant errors when estimating the energy storage capacity for electrode performance in supercapacitor applications. Despite the limitations, the 3-cell electrode configuration does allow users to study the electrochemical properties of the active material in the working electrode. In addition, the electrolyte and solvent stability could also be investigated.[102]

However, as most supercapacitors consist of a 2-electrode configuration, therefore, the test configuration should also be a 2-electrode configuration to ensure that results obtained in the test would truly reflect commercial applications. Unlike the 3-electrode configuration, the 2-electrode configuration consists of 2 working electrodes with potential differences applied to both electrodes being the same. This results in a specific capacitance that is slightly less than half of the 3-electrode configuration.[101,102]

Staiti and co-workers discovered that the measured specific capacitance of electrode active carbon materials depended greatly on electrode compositions and working conditions.[102] Therefore, it would be wise to conduct a test on the electrochemical performance of the material in question in a 3-electrode configuration and then follow it up with a 2-electrode configuration such that the researcher can get a clearer picture of how actual working conditions might influence the measured electrode performance in the 3-electrode configuration.

4.2 Physical properties of electrodes

Apart from the electrode cell configuration, the mass loading of the active material as well as the thickness of the electrode do play a role in electrode performance. For example, a higher energy density can be achieved with a thicker electrode while a higher power density can be achieved with a thinner electrode. Therefore, it is crucial that the electrode used for testing should be of comparable thickness to the actual commercial electrode so as to achieve accurate and comparable results. It is also known that electrodes that are very thin or have little active material tend to over-exaggerate their performance.[101]

The composition of the electrodes also plays an important role in accurately determining the electrode performance. For example, the active material used in the electrode must have a significantly higher capacitance compared to other cell components such as the binder and electrode support surface. This is to reduce the margin of errors that are caused by the capacitance contributed from these non-active materials in the electrode.[101]

4.3 Choice of electrolyte

In the current literature, the optimization of electrolyte has been elaborated as one of the pivotal components that is necessary to improve the supercapacitor performance.[24] Both the two key parameters of energy density and power density are affected by the types of electrolytes we use. For instance, the energy density is affected by the voltage window and ion concentration of the electrolyte while the power density is impacted by the resistance of the electrolyte.

Based on past and current research, 3 main types of electrolytes have been identified for use in supercapacitors. They are aqueous electrolytes, organic electrolytes and ionic liquid electrolytes. Often, salts are added to both aqueous and organic electrolytes to provide additional ionic conductivity in the full specified temperature range. For the specified range, the aqueous/organic electrolytes with salts must not freeze or evaporate and the salts must not precipitate. The salts must also be added in sufficient quantities (typically 1 M) to prevent any ionic depletion at high voltage.[103] Separately, ionic liquid electrolytes may be mixed with a solvent to reduce its viscosity and consequently increase its conductivity while reducing the series resistance. The choice of electrolytes depends on 4 parameters namely the resistance, capacitance, ease of production and potential window in which the electrolyte will remain stable.

Aqueous electrolyte. From the tables showing the summary of test results in the sections above, both organic and aqueous electrolytes are commonly used for testing the electrode performance. Common aqueous electrolytes include Na_2SO_4, KOH, H_2SO_4, and KCl. Notably, aqueous electrolytes were more commonly used than organic electrolytes in electrode testing scenarios. However, this phenomenon does not reflect the real-world situation as organic electrolytes are commonly applied in real-world supercapacitors because of their larger electrochemical window which grants the electrodes greater energy storage capacity.[101] Aqueous electrolytes, on the other hand, can only have electrochemical windows of up to 1 V due to the electrolytic decomposition of water. Additionally, the use of different types of electrolytes will result in different specific capacitance values obtained. For example, aqueous electrolytes used in SWCNT electrode test cells typically yield 40–50% higher capacitance values compared to organic electrolytes.[101]

Organic electrolytes. Common types of organic electrolytes include $TEABF_4$ in propylene carbonate. Shortcomings of organic electrolytes include depletion of the electrolyte upon charging, small operating temperature range and safety problems. In addition, organic electrolytes tend to exhibit larger resistance compared to aqueous electrolytes. This tends to result in the shape of the CV loop being non-rectangular. Organic electrolytes also tend to have poorer conductivities and it is necessary to keep the electrolyte away from contact with H_2O so as not to further weaken the conductivity or increase the resistance.[55] A possible reason for the weaker conductivity performance, compared to aqueous electrolytes, is that organic electrolytes tend to consist of bigger ions which may have difficulty accessing the micropores of the graphene sheet electrodes. However, this shortcoming tends to be compensated by the larger electrochemical window which allows for higher cell voltage, energy density and specific power density.[104]

Ionic liquid electrolytes. Ionic liquid electrolytes are non-volatile liquids that are rarely used but recent research suggests that their use may increase in the near future because of their favourable properties such as excellent thermal stability, conductivity, large electrochemical window and recyclability. In addition, the physical and chemical properties of the electrolyte can be managed by substituting for its cations, anions or substituents.[104] However, it was discovered in a study that due to the high viscosity of pure ionic liquids, ionic transfer would be impaired and organic solvents such as acetonitrile could be added to reduce the viscosity and thus improve the ionic conductivity. The study concluded that an addition of 25% acetonitrile to 75% $bmimPF_6$ result in an increased capacitance compared to pure $bmimPF_6$ while the electrochemical window remained relatively wide at 2.8 V.[104]

Another beneficial property of ionic liquid electrolytes is its ability to be used as an excellent surfactant in preventing the aggregation of graphene sheets. This is a result of weakening of the van der Waals forces between the graphene sheets by the ionic liquids thus allowing greater dispersion and distribution of these sheets which subsequently increase the accessibility of electrolytes.[105] This beneficial trait is most useful during the preparation of electrodes as the exposure of these electrodes to ionic liquids will increase the accessibility of ions and thus the capacitance.

In an interesting report, Liu and co-workers conducted further research into the synergistic effects between organic solvents and ionic liquid electrolytes. It was discovered that the electrochemical performance of graphene electrodes depended heavily on the types of functional groups in the organic solvents as well as the length of the alkyl group in the ionic liquid electrolyte.[106] In the study, 0.5 M $EMIMBF_4$ was used as the ionic liquid electrolyte and it was dissolved in organic solvents such as CH_2Cl_2, CH_3COOH, CH_3CN, C_3H_7NO and CH_3COCH_3. It was observed that the addition of the organic solvent caused the electrochemical window to decrease from 4 V to 1.9 V and this could also be due to the concentration of ionic liquid being reduced. In addition, the Nyquist plots of $EMIMBF_4/CH_3CN$, $EMIMBF_4/C_3H_7NO$ and $EMIMBF_4/CH_3COCH_3$ electrolytes showed lower resistance for charge transfer and equivalent series thus validating that these 3 organic solvents are more compatible with ionic liquid mixing. $EMIMBF_4/CH_2Cl_2$ and $EMIMBF_4/CH_3CH_2COOH$ electrolytes were not ideal as they experience the "ionic absent effect".[107] Further tests by CV and galvanostatic charge–discharge revealed ideal EDLC even at a high scan rate of 50 mV s^{-1} with $EMIMBF_4/C_3H_7NO$ exhibiting the highest specific capacitance of 90.6 F g^{-1}.[106]

Liu and co-workers' research also revealed that the longer the length of the alkyl group in ionic liquid solvents, the lower the conductivity and thus the capacitance. By using the same organic solvent, C_3H_7NO, in ionic liquids ($MMIMBF_4$, $EMIMBF_4$, and $BMIMBF_4$) with varying alkyl group lengths, it was observed that the $BMIMBF_4/C_3H_7NO$ electrolyte achieved the highest capacitance at 95.3 F g^{-1} due to its short alkyl group. However, it should be noted that the difference in capacitance is negligible as the difference in chain lengths is not significant.[106]

4.4 Measurement methodology

Measurement methodologies for charging rates, voltage ranges and calculation of parameters such as specific capacitance will affect electrode performance results and should thus follow certain established procedures. As energy density, which is related to the specific capacitance, is currently the most important parameter that researchers are trying to improve,

therefore, measurement methods for the specific capacitance play an important role. Specific capacitance of a cell can be determined by galvanostatic/constant current discharge curves (CC curves) or cyclic voltammetry curves (CV). Presently, CC curves are the conventional measurement method for measuring the capacitance of packaged supercapacitors in the industry and this method is highly dependent on how the loading is applied to the supercapacitor. Using the charge–discharge method, the specific capacitance can be calculated *via* the equation below.

$$C = \frac{I}{m\mathrm{d}v/\mathrm{d}t} \quad (4)$$

where I represents the discharge current, m represents the electrode's active material mass and $(\mathrm{d}v/\mathrm{d}t)$ represents the discharge curve's slope. It is suggested that 2 reference points be used to calculate the slope of the discharge curve $(\mathrm{d}v/\mathrm{d}t)$ especially since the nonlinear response is possible due to faradaic reactions. In general, the 2 reference points used correspond to the time at maximum and half the maximum voltage respectively.[108]

CV curves, on the other hand, depend on the scan rate, voltage range and computation methods.[101] The average capacitance can be calculated from the CV curve *via* the following equation below.

$$C(F/g) = \frac{1}{2mVv}\int_{V^-}^{V^+} I(V)\mathrm{d}V \quad (5)$$

In the equation, Q(C) represents the sum of charges obtained *via* integration of the positive and negative sweeps in the CV curve. 'm' (g) represents active material's mass in the electrodes, v (V s^{-1}) signifies the scan rate and indicates the potential window between the 2 electrodes. CV curves typically exhibit a rectangular shape conformation when the capacitance originates *via* the electric double layer pathway. However, if faradaic reactions occur, redox peaks would appear in the CV curve thus disrupting the rectangular shape.[108]

For the reporting of specific capacitance values *via* the CV or CC curves, it is imperative that the scan rate (for CV curves) or current density (for CC curves) be reported as well. This is because the values obtained for specific capacitance are dependent on the scan rate or current density used. It is generally known that the highest specific capacitance can be obtained at low scan rates or current densities but this would also reflect poor rate capabilities and might not reflect the actual performance of the supercapacitor in commercial applications.

Apart from the specific capacitance, another important parameter that determines superior capacitor performance is the minimal equivalent series resistance (ESR). To evaluate the magnitude of ESR in a supercapacitor, a linear fit of the IR drop values obtained from the CC curves at different current densities could be used.

Additionally, the voltage range applied to testing should match 2 criteria. The first criterion is that the voltage range should be similar to the range that is being used in the commercial applications. The second criterion is that the voltage range must match the electrolyte's electrochemical window. Notably, application of a voltage range above the operating voltage threshold of a cell will lead to deterioration in efficiency and lifetime of the cell due to non-reversible reactions in the cell.[101]

Low discharge rates would also likely lead to big error margins especially if the electrode mass is small. This is due to the 'noise' created by the capacitance produced from other cell components as well as current leakage. Furthermore, adjustment should be made to the current to provide a charge–discharge timing of 5–60 seconds.[101]

5 Conclusion

There has been much progress in the field of graphene electrochemical energy storage and conversion devices such as the increasing research into how graphene could be combined with metal oxides and conducting polymers to produce hybrids with excellent electrochemical properties. Despite this, more work must be done to understand how the structure of these metal oxide–polymers and their interactions with graphene bring about such synergistic effects. This could be done by systematically varying these factors while at the same time studying their impacts. This will allow us to reconcile experimental results with first principles which will assist in our understanding of graphene materials as a whole. Such an understanding is important as it will ensure that we can tune materials in future to attain the maximum possible electrochemical performance for supercapacitor applications.

In addition, as described in this literature review, many factors such as electrode thickness, the number of graphene layers and structure affect its electrochemical performance. Therefore, more research must be conducted to develop synthesis methods that would allow easy control for producing graphene with the desired structure.

Lastly, it is important to use the appropriate test-cell configuration and electrode design to ensure that tests conducted accurately reflect actual commercial applications. Measurement methodologies also vary widely and an industry-wide standardization would be useful in helping with result analysis.

Acknowledgements

We wish to acknowledge the funding support for this project from Nanyang Technological University under the Undergraduate Research Experience on CAmpus (URECA) programme.

References

1 D. R. Dreyer, R. S. Ruoff and C. W. Bielawski, From Conception to Realization: An Historial Account of Graphene and Some Perspectives for Its Future, *Angew. Chem., Int. Ed.*, 2010, **49**, 9336–9344.
2 H. P. Boehm, R. Setton and E. Stumpp, Nomenclature and Terminology of Graphite Intercalation Compounds, *Carbon*, 1986, **24**, 241.
3 R. K. Kalyoncu and H. A. Taylor, Jr, in *Kirk-Othmer Encyclopedia of Chemical Technology*, Wiley, Hoboken, 5th edn, 2005, vol. 12, p. 771.

4 H.-P. Boehm and E. Stumpp, Citation errors concerning the first report on exfoliated graphite, *Carbon*, 2007, **45**, 1381.
5 C. Schafhaeutl, Ueber die Verbindungen des Kohlenstoffes mit Silicium, Eisen und anderen Metallen, welche die verschiedenen Gattungen von Roheisen, Stahl und Schmiedeeisen bilden, *J. Prakt. Chem.*, 1840, **21**, 129.
6 B. C. Brodie, On the Atomic Weight of Graphite, *Philos. Trans. R. Soc., A*, 1859, **149**, 249.
7 D. R. Dreyer, S. Park, C. W. Bielawski and R. S. Ruoff, The Chemistry of Graphene Oxide, *Chem. Soc. Rev.*, 2010, **39**, 228.
8 G. Ruess and F. Vogt, Höchstlamellarer Kohlenstoff aus Graphitoxyhydroxyd, *Monatsh. Chem.*, 1948, **78**, 222.
9 H. P. Boehm, A. Clauss, G. O. Fischer and U. Hofmann, Adsorption Behaviors of Extremely Thin Carbon Foils, *Z. Anorg. Allg. Chem.*, 1962, **316**, 119.
10 J. T. Grant and T. W. Haas, A study of Ru(0001) and Rh(111) surfaces using LEED and Auger electron spectroscopy, *Surf. Sci.*, 1970, **21**, 76.
11 J. M. Blakely, J. S. Kim and H. C. Potter, Segregation of Carbon to the (100) Surface of Nickel, *J. Appl. Phys.*, 1970, **41**, 2693.
12 A. J. van Bommel, J. E. Crombeen and A. van Tooren, LEED and Auger electron observations of the SiC(0001) surface, *Surf. Sci.*, 1975, **48**, 463.
13 A. Nagashima, K. Nuka, K. Satoh, H. Itoh, T. Ichinokawa, C. Oshima and S. Otani, Electronic structure of monolayer graphite on some transition metal carbide surfaces, *Surf. Sci.*, 1993, **287**, 609.
14 A. Affoune, B. Prasad, H. Sato, T. Enoki, Y. Kaburagi and Y. Hishiyama, Experimental evidence of a single nano-graphene, *Chem. Phys. Lett.*, 2001, **348**, 17.
15 K. Seibert, G. C. Cho, W. Kütt, H. Kurz, D. H. Reitze, J. I. Dadap, H. Ahn, M. C. Downer and A. M. Malvezzi, Femtosecond Carrier Dynamics in Graphite, *Phys. Rev. B: Condens. Matter Mater. Phys.*, 1990, **42**, 2842.
16 K. S. Novoselov, A. K. Geim, S. V. Morozov, D. Jiang, Y. Zhang, S. V. Dubonos, I. V. Grigorieva and A. A. Firsov, Electric field effect in atomically thin carbon films, *Science*, 2004, **306**, 666.
17 T. W. Ebbesen and H. Hiura, Graphene in 3-dimensions—towards graphite origami, *Adv. Mater.*, 1995, **7**, 582.
18 X. Lu, M. Yu, H. Huang and R. S. Ruoff, Tailoring graphite with the goal of achieving single sheets, *Nanotechnology*, 1999, **10**, 269.
19 Y. Gan, W. Chu and L. Qiao, STM investigation on interaction between superstructure and grain boundary in graphite, *Surf. Sci.*, 2003, **539**, 120.
20 A. K. Geim, Graphene prehistory, *Phys. Scr., T*, 2012, **146**, 014003.
21 J. Hou, Y. Shao, M. W. Ellis, R. B. Moored and B. Yie, Graphene-based electrochemical energy conversion and storage: fuel cells, supercapacitors and lithium ion batteries, *Phys. Chem. Chem. Phys.*, 2011, **13**, 15384–15402.
22 B. E. Conway, *Electrochemical Supercapacitors: Scientific Fundamentals and Technological Applications*, Springer, 1999.
23 P. Simon and Y. Gogotsi, Materials for electrochemical capacitors, *Nat. Mater.*, 2008, **7**, 845–854.
24 M. S. Halper and J. C. Ellenbogen, *Supercapacitors: A Brief Overview*, MITRE Nanosystems Group, 2006.
25 S. D. Perera, R. G. Mariano, N. Nijem, Y. Chabal, J. P. Ferraris and K. J. Balkus Jr, Alkaline deoxygenated graphene oxide for supercapacitor applications: An effective green alternative for chemically reduced graphene, *J. Power Sources*, 2012, **215**, 1e10.
26 Jaidev and S. Ramaprabhu, Poly(*p*-phenylenediamine)/graphene nanocomposites for supercapacitor applications, *J. Mater. Chem.*, 2012, **22**, 18775.
27 S. Park and R. S. Ruoff, Chemical methods for the production of graphenes, 2009, **4**, 217–224.
28 R. S. Edwards and K. S. Coleman, Graphene synthesis: relationship to applications, *Nanoscale*, 2013, **5**, 38–51.
29 C. Xu, B. Xu, Y. Gu, Z. Xiong, J. Sun and X. S. Zhao, Graphene-based electrodes for electrochemical energy storage, *Energy Environ. Sci.*, 2013, **6**, 1388.
30 D. Zhang, X. Zhang, Y. Chen, C. Wang and Y. Ma, An environment-friendly route to synthesize reduced graphene oxide as a supercapacitor electrode material, *Electrochim. Acta*, 2012, **69**, 364–370.
31 J. Chen, M. Duan and G. Chen, Continuous mechanical exfoliation of graphene sheets *via* three-roll mill, *J. Mater. Chem.*, 2012, **22**, 19625.
32 S. Stankovich, D. A. Dikin, R. D. Piner, K. A. Kohlhaas, A. Kleinhammes, Y. Jia, Y. Wu, S. T. Nguyen and R. S. Ruoff, Synthesis of graphene-based nanosheets *via* chemical reduction of exfoliated graphite oxide, *Carbon*, 2007, **45**, 1558.
33 G. Eda, G. Fanchini and M. Chhowalla, Large-area ultrathin films of reduced graphene oxide as a transparent and flexible electronic material, *Nat. Nanotechnol.*, 2008, **3**, 270.
34 C. Gomez-Navarro, R. T. Weitz, A. M. Bittner, M. Scolari, A. Mews, M. Burghard and K. Kern, Electronic Transport Properties of Individual Chemically Reduced Graphene Oxide Sheets, *Nano Lett.*, 2007, **7**, 3499.
35 H. Kang, A. Kulkarni, S. Stankovich, R. S. Ruoff and S. Baik, Restoring electrical conductivity of dielectrophoretically assembled graphite oxide sheets by thermal and chemical reduction techniques, *Carbon*, 2009, **47**, 1520.
36 J. N. Coleman, Liquid-Phase Exfoliation of Nanotubes and Graphene, *Adv. Funct. Mater.*, 2009, **19**, 3680–3695.
37 M. Lotya, Y. Hernandez, P. J. King, R. J. Smith, V. Nicolosi, L. S. Karlsson, F. M. Blighe, S. De, Z. Wang, I. T. McGovern, G. S. Duesberg and J. N. Coleman, Liquid Phase Production of Graphene by Exfoliation of Graphite in Surfactant/Water Solutions, *J. Am. Chem. Soc.*, 2009, **131**, 3611.
38 J. Coraux, *et al.*, Structural coherency of graphene on Ir(111), *Nano Lett.*, 2008, **8**(2), 565–570.
39 P. W. Sutter, J. I. Flege and E. A. Sutter, Epitaxial graphene on ruthenium, *Nat. Mater.*, 2008, **7**(5), 406–411.
40 X. Cao, Y. Shi, W. Shi, G. Lu, X. Huang, Q. Yan, Q. Zhang and H. Zhang, Preparation of Novel 3D Graphene Networks for Supercapacitor Applications, *Small*, 2011, **7**(no. 22), 3163–3168.

41 B. Hu, H. Ago, Y. Ito, K. Kawahara, M. Tsuji, E. Magome, K. Sumitani, N. Mizuta, K.-i. Ikeda and S. Mizuno, Epitaxial growth of large-area single-layer graphene over Cu(111)/sapphire by atmospheric pressure CVD, *Carbon*, 2012, **50**, 57–65.

42 M. Gao, Y. Pan, L. Huang, H. Hu, L. Z. Zhang, H. M. Guo, S. X. Du and H.-J. Gao, Epitaxial growth and structural property of graphene on Pt(111), *Appl. Phys. Lett.*, 2011, **98**, 033101.

43 H. Huang, S. Liang Wong, C.-C. Tin, Z. Qiang Luo, Z. Xiang Shen, W. Chen and A. T. S. Wee, Epitaxial growth and characterization of graphene on free-standing polycrystalline 3C-SiC, *J. Appl. Phys.*, 2011, **110**, 014308.

44 S. Stankovich, *et al.*, Synthesis of graphene-based nanosheets via chemical reduction of exfoliated graphite oxide, *Carbon*, 2007, **45**(7), 1558–1565.

45 S. D. Perera, R. G. Mariano, N. Nijem, Y. Chabal, J. P. Ferraris and K. J. Balkus Jr, Alkaline deoxygenated graphene oxide for supercapacitor applications: An effective green alternative for chemically reduced graphene, *J. Power Sources*, 2012, **215**, 1e10.

46 R. Chen, S. Yu, R. Sun, W. Yang and Y. Zhao, KCl-assisted, chemically reduced graphene oxide for high-performance supercapacitor electrodes, *J. Solid State Electrochem.*, 2012, **16**, 3635–3641.

47 B. Zhao, P. Lia, Y. Jiang, D. Pan, H. Tao, J. Song, T. Fang and W. Xu, Supercapacitor performances of thermally reduced graphene oxide, *J. Power Sources*, 2012, **198**, 423–427.

48 D. Sun, X. Yan, J. Lang and Q. Xue, High performance supercapacitor electrode based on graphene paper *via* flame-induced reduction of graphene oxide paper, *J. Power Sources*, 2013, **222**, 52e58.

49 X.-Y. Peng, X.-X. Liu, D. Diamond and K. T. Lau, Synthesis of electrochemically-reduced graphene oxide film with controllable size and thickness and its use in supercapacitor, *Carbon*, 2011, **49**, 3488–3496.

50 A. G. Cano-Márquez, F. J. Rodríguez-Macías, J. Campos-Delgado, C. G. Espinosa-González, F. Tristán-López, D. Ramírez-González, D. A. Cullen, D. J. Smith, M. Terrones and Y. I. Vega-Cantu, Ex-MWNTs: Graphene Sheets and Ribbons Produced by Lithium Intercalation and Exfoliation of Carbon Nanotubes, *Nano Lett.*, 2009, **9**(4), 1527–1533.

51 D. V. Kosynkin, A. L. Higginbotham, A. Sinitskii, J. R. Lomeda, A. Dimiev, B. Katherine Price and J. M. Tour, Longitudinal unzipping of carbon nanotubes to form graphene nanoribbons, 2009, **458**, 872–876.

52 M. Seredych, M. Koscinski, M. Sliwinska-Bartkowiak and T. J. Bandosz, Active pore space utilization in nanoporous carbon-based supercapacitors: effects of conductivity and pore accessibility, *J. Power Sources*, 2012, **220**, 243e252.

53 M. Seredych, R. Chen and T. J. Bandosz, Effects of the addition of graphite oxide to the precursor of a nanoporous carbon on the electrochemical performance of the resulting carbonaceous composites, *Carbon*, 2012, **50**, 4144–4154.

54 L. T. Le, M. H. Ervin, H. Qiu, B. E. Fuchs and W. Y. Lee, Graphene supercapacitor electrodes fabricated by inkjet printing and thermal reduction of graphene oxide, *Electrochem. Commun.*, 2011, **13**, 355–358.

55 Q. Cheng, J. Tang, J. Ma, H. Zhang, N. Shinya and L.-C. Qinc, Graphene and carbon nanotube composite electrodes for supercapacitors with ultra-high energy density, *Phys. Chem. Chem. Phys.*, 2011, **13**, 17615–17624.

56 Q. Cheng, J. Tang, J. Ma, H. Zhang, N. Shinya and L. C. Qin, Graphene and nanostructured MnO_2 composite electrodes for supercapacitors, *Carbon*, 2011, **49**, 2917–2925.

57 L. Buglione and M. Pumera, Graphene/carbon nanotube composites not exhibiting synergic effect for supercapacitors: the resulting capacitance being average of capacitance of individual components, *Electrochem. Commun.*, 2012, **17**, 45–47.

58 M. Matsushima, M. Noda, G. Kalita, H. Uchida, K. Wakita and M. Umeno, Formation of graphene-containing porous carbon film for electric double-layer capacitor by pulsed plasma chemical vapor deposition, *Jpn. J. Appl. Phys.*, 2012, **51**, 045103.

59 Z. Lei, N. Christov, L. L. Zhang and X. S. Zhao, Mesoporous carbon nanospheres with an excellent electrocapacitive performance, *J. Mater. Chem.*, 2011, **21**, 2274.

60 Y.-S. Kim, K. Kumar, F. T. Fisher and E.-H. Yang, Out-of-plane growth of CNTs on graphene for supercapacitor applications, *Nanotechnology*, 2012, **23**, 015301.

61 Z. J. Li, B. C. Yang, S. R. Zhang and C. M. Zhao, Graphene oxide with improved electrical conductivity for supercapacitor electrodes, *Appl. Surf. Sci.*, 2012, **258**, 3726–3731.

62 J. Yan, J. Liu, Z. Fan, T. Wei and L. Zhang, High-performance supercapacitor electrodes based on highly corrugated graphene sheets, *Carbon*, 2012, **50**, 2179–2188.

63 Y. Li, M. v. Zijll, S. Chiang and N. Pana, KOH modified graphene nanosheets for supercapacitor electrodes, *J. Power Sources*, 2011, **196**, 6003–6006.

64 H.-C. Hsu, C.-H. Wang, S. K. Nataraj, H.-C. Huang, H.-Y. Du, S.-T. Chang, L.-C. Chen and K.-H. Chen, Stand-up structure of graphene-like carbon nanowalls on CNT directly grown on polyacrylonitrile-based carbon fiber paper as supercapacitor, *Diamond Relat. Mater.*, 2012, **25**, 176–179.

65 K. Zhang, L. Mao, L. L. Zhang, H. S. O. Chan, X. S. Zhao and J. Wu, Surfactant-intercalated, chemically reduced graphene oxide for high performance supercapacitor electrodes, *J. Mater. Chem.*, 2011, **21**, 7302.

66 K. Zhang, L. L. Zhang, X. S. Zhao and J. S. Wu, Graphene/Polyaniline Nanofibers Composites as Supercapacitor Electrodes, *Chem. Mater.*, 2010, **22**, 1392.

67 A. Yu, I. Roes, A. Davies and Z. Chen, Ultrathin, transparent, and flexible graphene films for supercapacitor application, *Appl. Phys. Lett.*, 2010, **96**, 253105.

68 J. Lin, J. Zhong, D. bao, J. Reiber-kyle, W. Wang, V. Vullev, M. Ozkan and C. S. Ozkan, *Electrochemical supercapacitor based on flexible pillar graphene nanostructures*, 978-1-61284-244- ©2011 IEEE, 2011.

69 P. Chen, J.-J. Yang, S.-S. Li, Z. Wang, T.-Y. Xiao, Y.-H. Qian and S.-H. Yu, Hydrothermal synthesis of macroscopic

nitrogen-doped graphene hydrogels for ultrafast supercapacitor, *Nano Energy*, 2013, **2**, 249–256.

70 Y. Liu, R. Deng, Z. Wang and H. Liu, Carboxyl-functionalized graphene oxide–polyaniline composite as a promising supercapacitor material, *J. Mater. Chem.*, 2012, **22**, 13619.

71 L. Lai, H. Yang, L. Wang, B. K. Teh, J. Zhong, H. Chou, L. Chen, W. Chen, Z. Shen, R. S. Ruoff and J. Lin, Preparation of Supercapacitor Electrodes through Selection of Graphene Surface Functionalities, *ACS Nano*, 2012, **6**(7), 5941–5951.

72 S. Biswas and L. T. Drzal, Multi Layered Nanoarchitecture of Graphene Nanosheets and Polypyrrole Nanowires forHigh Performance Supercapacitor Electrodes, *Chem. Mater.*, 2010, **22**, 5667.

73 S. Bose, N. H. Kim, T. Kuila, K. T. Lau and J. H. Lee, Electrochemical performance of a graphene–polypyrrole nanocomposite as a supercapacitor electrode, *Nanotechnology*, 2011, **22**, 295202.

74 J. Liu, J. An, Y. Ma, M. Li and R. Ma, Synthesis of a Graphene–Polypyrrole Nanotube Composite and Its Application in Supercapacitor Electrode, *J. Electrochem. Soc.*, 2012, **159**(6), A828–A833.

75 Z. Tai, X. Yan and Q. Xue, Shape-alterable and -recoverable graphene/polyurethane bi-layered composite film for supercapacitor electrode, *J. Power Sources*, 2012, **213**, 350e357.

76 L. L. Zhang, S. Zhao, X. N. Tian and X. S. Zhao, Layered Graphene Oxide Nanostructures with Sandwiched Conducting Polymers as Supercapacitor Electrodes, *Langmuir*, 2010, **26**(22), 17624–17628.

77 H. Liua, Y. Wang, X. Gou, T. Qi, J. Yang and Y. Ding, Three-dimensional graphene/polyaniline composite material for high-performance supercapacitor applications, *Mater. Sci. Eng., B*, 2013, **178**, 293–298.

78 L. L. Zhang, R. Zhou and X. S. Zhao, Graphene-based materials as supercapacitor electrodes, *J. Mater. Chem.*, 2010, **20**, 5983.

79 J. R. Lake, A. Cheng, S. Selverston, Z. Tanaka, J. Koehne, *et al.*, Graphene metal oxide composite supercapacitor electrodes, *J. Vac. Sci. Technol., B: Nanotechnol. Microelectron.: Mater., Process., Meas., Phenom.*, 2012, **30**, 03D118.

80 W. Yang, Z. Gao, J. Wang, B. Wang, Q. Liu, Z. Li, T. Mann, P. Yang, M. Zhang and L. Liu, Synthesis of reduced graphene nanosheet/urchin-like manganese dioxide composite and high performance as supercapacitor electrode, *Electrochim. Acta*, 2012, **69**, 112–119.

81 Jaidev, R. I. Jafri, S. Ramaprabhu, *Hydrothermal synthesis of $RuO_2 \cdot xH_2O$/graphene hybrid nanocomposite for supercapacitor application*, 978-1-4577-2037-6/11/$26.00 ©2011 IEEE, 2011.

82 J. P. Zheng, P. J. Cygan and T. R. Jow, Hydrous Ruthenium Oxide as an Electrode Material for Electrochemical Capacitors, *J. Electrochem. Soc.*, 1995, **142**(8).

83 J. Woo Lee, A. S. Hall, J.-D. Kim and T. E. Mallouk, A Facile and Template-Free Hydrothermal Synthesis of Mn_3O_4 Nanorods on Graphene Sheets for Supercapacitor Electrodes with Long Cycle Stability, *Chem. Mater.*, 2012, **24**, 1158–1164.

84 S. L. Brock, N. Duan, Z. R. Tian, O. Giraldo, H. Zhou and S. L. Suib, A review of porous manganese oxide materials, *Chem. Mater.*, 1998, **10**, 2619.

85 J. Yan, Z. Fan, T. Wei, W. Qian, M. Zhang and F. Wei, Fast and reversible surface redox reaction of graphene–MnO_2 composites as supercapacitor electrodes, *Carbon*, 2010, **48**, 3825–3833.

86 Z. Lei, F. Shi and L. Lu, Incorporation of MnO_2-Coated Carbon Nanotubes between Graphene Sheets as Supercapacitor Electrode, *ACS Appl. Mater. Interfaces*, 2012, **4**, 1058–1064.

87 W. Zhou, J. Liu, T. Chen, K. Seng Tan, X. Jia, Z. Luo, C. Cong, H. Yang, C. Ming Lic and T. Yu, Fabrication of Co_3O_4-reduced graphene oxide scrolls for high-performance supercapacitor electrodes, *Phys. Chem. Chem. Phys.*, 2011, **13**, 14462–14465.

88 X. Xia, J. Tu, Y. Mai, R. Chen, X. Wang, C. Gu and X. Zhao, Graphene Sheet/Porous NiO Hybrid Film for Supercapacitor Applications, *Chem.–Eur. J.*, 2011, **17**, 10898–10905.

89 C. Xiang, M. Li, M. Zhi, A. Manivannanc and N. Wu, Reduced graphene oxide/titanium dioxide composites for supercapacitor electrodes: shape and coupling effects, *J. Mater. Chem.*, 2012, **22**, 19161.

90 N. Q. Wu, J. Wang, D. Tafen, H. Wang, J.-G. Zheng, J. P. Lewis, X. Liu, S. S. Leonard and A. Manivannan, Shape-enhanced photocatalytic activity of single-crystalline anatase TiO(2) (101) nanobelts, *J. Am. Chem. Soc.*, 2010, **132**, 6679.

91 M. Zhi, S. Lee, N. Miller, N. H. Menzler and N. Q. Wu, An intermediate-temperature solid oxide fuel cell with electrospun nanofiber cathode, *Energy Environ. Sci.*, 2012, **5**, 7066.

92 D. Wang, H. Zhao, N. Q. Wu, A. El Khakani and D. Ma, Tuning the Charge-Transfer Property of PbS-Quantum Dot/TiO_2-Nanobelt Nanohybrids *via* Quantum Confinement, *J. Phys. Chem. Lett.*, 2010, **1**, 1030.

93 G. Yu, L. Hu, N. Liu, H. Wang, M. Vosgueritchian, Y. Yang, Y. Cui and Z. Bao, Enhancing the Supercapacitor Performance of Graphene/MnO_2 Nanostructured Electrodes by Conductive Wrapping, *Nano Lett.*, 2011, **11**, 4438–4442.

94 J. Yuan, J. Zhu, H. Bi, Z. Zhang, S. Chen, S. Liang and X. Wang, Self-assembled hydrothermal synthesis for producing a $MnCO_3$/graphene hydrogel composite and its electrochemical properties, *RSC Adv.*, 2013, **3**, 4400.

95 X. Huang, Z. Zeng, Z. Fan, J. Liu and H. Zhang, Graphene-Based Electrodes, *Adv. Mater.*, 2012, **24**, 5979–6004.

96 J. Zhang, J. Jiang, H. Lib and X. S. Zhao, A high-performance asymmetric supercapacitor fabricated with graphene-based electrodes, *Energy Environ. Sci.*, 2011, **4**, 4009.

97 Z.-S. Wu, W. Ren, D.-W. Wang, F. Li, B. Liu and H.-M. Cheng, High-Energy MnO_2 Nanowire/Graphene and Graphene Asymmetric Electrochemical Capacitors, *ACS Nano*, 2010, **4**(10), 5835–5842.

98 J. Yan, Z. Fan, W. Sun, G. Ning, T. Wei, Q. Zhang, R. Zhang, L. Zhi and F. Wei, Advanced Asymmetric Supercapacitors Based on $Ni(OH)_2$/Graphene and Porous Graphene Electrodes with High Energy Density, *Adv. Funct. Mater.*, 2012, **22**, 2632–2641.

99 Z. Fan, J. Yan, T. Wei, L. Zhi, G. Ning, T. Li and F. Wei, Asymmetric Supercapacitors Based on Graphene/MnO_2 and Activated Carbon Nanofiber Electrodes with High Power and Energy Density, *Adv. Funct. Mater.*, 2011, **21**, 2366–2375.

100 P. Tang, Y. Zhao, C. Xu and K. Ni, Enhanced energy density of asymmetric supercapacitors *via* optimizing negative electrode material and mass ratio of negative/positive electrodes, *J. Solid State Electrochem.*, 2013, **17**, 1701–1710.

101 M. D. Stoller and R. S. Ruoff, Best practice methods for determining an electrode material's performance for ultracapacitors, *Energy Environ. Sci.*, 2010, **3**, 1294–1301.

102 P. Staiti and F. Lufrano, A study of the electrochemical behaviour of electrodes in operating solid-state supercapacitors, *Electrochim. Acta*, 2007, **53**, 710–719.

103 J. P. Zheng and T. R. Jow, The effect of salt concentration in electrolytes on the maximum energy storage for double layer capacitors, *J. Electrochem. Soc.*, 1997, **144**(7), 2417–2420.

104 C. Fu, Y. Kuang, Z. Huang, X. Wang, Y. Yin, J. Chen and H. Zhou, Supercapacitor based on graphene and ionic liquid electrolyte, *J. Solid State Electrochem.*, 2011, **15**, 2581–2585.

105 P. Tamilarasan, A. Kumar Mishra and S. Ramaprabhu, *Graphene/Ionic Liquid Binary Electrode Material for High Performance Supercapacitor*, 978-1-4577-2037-6/11/$26.00 ©2011 IEEE, 2011.

106 W. Liu, X. Yan, J. Lang and Q. Xue, Electrochemical behavior of graphene nanosheets in alkylimidazolium tetrafluoroborate ionic liquid electrolytes: influences of organic solvents and the alkyl chains, *J. Mater. Chem.*, 2011, **21**, 13205.

107 W. G. Pell and B. E. Conway, Analysis of power limitations at porous supercapacitor electrodes under cyclic voltammetry modulation and dc charge, *J. Power Sources*, 2001, **96**, 57.

108 J. R. Miller and A. F. Burke, *Electrochemical Capacitors: Challenges and Opportunities for Real-World Applications*, The Electrochemical Society Interface, 2008.